

Superallowed $0^+ \rightarrow 0^+$ nuclear β -decays:

A critical survey with tests of CVC and the standard model

J.C. Hardy^{1,*} and I.S. Towner^{1,2}

¹*Cyclotron Institute, Texas A&M University, College Station, Texas 77843*

²*Physics Department, Queen's University,
Kingston, Ontario K7L 3N6, Canada*

(Dated: October 22, 2018)

Abstract

A complete and critical survey is presented of all half-life, decay-energy and branching-ratio measurements related to 20 superallowed $0^+ \rightarrow 0^+$ decays; no measurements are ignored, though some are rejected for cause and others updated. A new calculation of the statistical rate function f is described and experimental ft values determined. The associated theoretical corrections needed to convert these results into $\mathcal{F}t$ values are discussed, and careful attention is paid to the origin and magnitude of their uncertainties. As an exacting confirmation of the conserved vector current hypothesis, the $\mathcal{F}t$ values are seen to be constant to 3 parts in 10^4 . These data are also used to set a new limit on any possible scalar interaction: $C_S/C_V = -(0.00005 \pm 0.00130)$. The average $\mathcal{F}t$ value obtained from the survey, when combined with the muon lifetime, yields the up-down quark-mixing element of the Cabibbo-Kobayashi-Maskawa matrix, $V_{ud} = 0.9738 \pm 0.0004$; and the unitarity test on the top row of the matrix becomes $|V_{ud}|^2 + |V_{us}|^2 + |V_{ub}|^2 = 0.9966 \pm 0.0014$ using the Particle Data Group's currently recommended values for V_{us} and V_{ub} . We also express this result in terms of the possible existence of right-hand currents. Finally, we discuss the priorities for future theoretical and experimental work with the goal of making the CKM unitarity test more definitive.

PACS numbers: 23.40.Bw, 12.15.Hh, 12.60.-i

*Electronic address: hardy@comp.tamu.edu

I. INTRODUCTION

Precise measurements of the beta decay between nuclear analog states of spin, $J^\pi = 0^+$, and isospin, $T = 1$, provide demanding and fundamental tests of the properties of the electroweak interaction. Collectively, these transitions can sensitively probe the conservation of the vector weak current, set tight limits on the presence of scalar or right-hand currents and contribute to the most demanding available test of the unitarity of the Cabibbo-Kobayashi-Maskawa (CKM) matrix, a fundamental tenet of the electroweak standard model.

Eight transitions, ^{14}O , $^{26}\text{Al}^m$, ^{34}Cl , $^{38}\text{K}^m$, ^{42}Sc , ^{46}V , ^{50}Mn and ^{54}Co are particularly amenable to experiment and, because of their significance to physics, have consequently received a good deal of attention over the past few decades. In each of these cases, the experimental ft -value is known to better than 0.1%. In the 1990s, ^{10}C was added to this list; its ft value is known to a precision of 0.15%. More recently, three more cases have been added: ^{22}Mg , ^{34}Ar and ^{74}Rb , with ft -value standard deviations ranging from from 0.24% to 0.40%. In the near future these uncertainties will undoubtedly be reduced and an additional eight cases could well be added to the list. Though improvements are still possible, with current data we can test the conserved vector current hypothesis at the level of 3 parts in 10^4 and the three-generation Standard Model at the level of its quantum corrections.

Over the past decade, it has become increasingly clear that the CKM unitarity test made possible by these measurements does not, in fact, quite agree with standard-model expectations. The test involves the top row of the CKM matrix and requires that the sum of squares of the three experimentally-determined elements, $|V_{ud}|^2 + |V_{us}|^2 + |V_{ub}|^2$, should equal 1. With results from superallowed β -decay providing the input for V_{ud} , and values for V_{us} and V_{ub} taken from the Particle Data Group reviews, the sum falls short of unity by 0.3%, more than twice the quoted standard deviation [1] – a provocative but hardly definitive disagreement. Nevertheless, it has stimulated experimental activity not only on the nuclear decays used to determine V_{ud} but also on the K_{e3} branching ratio used for V_{us} . Strikingly, a new measurement of the K_{e3}^+ branching ratio [2] has thrown the accepted value of V_{us} into doubt. Although the new branching-ratio result disagrees significantly with previous measurements, it would, if taken by itself, lead to a larger value for V_{us} and thus bring the CKM top-row sum into agreement with unity. At this time, the value of V_{us} remains controversial and there are a number of kaon-decay experiments currently underway, which

should lead to a settled outcome within a very few years.

With all this activity in progress, and the likelihood that a new and reliable value of V_{us} will soon be forthcoming, this is an opportune time to produce a complete new survey of the nuclear data used to establish V_{ud} . This way, we will be able to view the value of V_{ud} with renewed confidence in anticipation of a revised result for V_{us} . (V_{ub} is very small and contributes a negligible .001% to the unitarity sum.) We have published four previous surveys, refs. [3, 4, 5, 6]: the most recent appeared fifteen years ago and included only eight superallowed transitions. In addition to bringing the results for these cases up to date, we are now incorporating data on twelve more transitions and have continued the practice we began in 1984 [5] of updating all original data to take account of the most modern calibration standards. We have also made completely new calculations of the statistical rate function, f , and employed the most complete radiative and isospin-symmetry-breaking corrections in dealing with the ft -values in the context of fundamental weak-interaction tests.

Superallowed Fermi beta decay between 0^+ states depends uniquely on the vector part of the hadronic weak interaction. When it occurs between isospin $T = 1$ analog states, the conserved vector current (CVC) hypothesis indicates that the ft values should be the same irrespective of the nucleus, *viz.*

$$ft = \frac{K}{G_V^2 |M_F|^2} = \text{constant}, \quad (1)$$

where $K/(\hbar c)^6 = 2\pi^3 \hbar \ln 2 / (m_e c^2)^5 = (8120.271 \pm 0.012) \times 10^{-10} \text{ GeV}^{-4}\text{s}$, G_V is the vector coupling constant for semi-leptonic weak interactions, and M_F is the Fermi matrix element, which for $T = 1$ states has the value $M_F = \sqrt{2}$. The CVC hypothesis asserts that the vector coupling constant, G_V , is a true constant and not renormalised to another value in the nuclear medium. A demonstration with the data assembled here that the ft values are indeed constant would provide a stringent test of the CVC hypothesis.

Unfortunately, Eq. (1) has to be amended slightly. Firstly, there are radiative corrections because, for example, the emitted electron may emit a bremsstrahlung photon, which goes undetected in the experiment. Secondly, isospin is not an exact symmetry in nuclei so the nuclear matrix element, M_F is slightly reduced from its ideal value, leading us to write: $|M_F|^2 = 2(1 - \delta_C)$. Thus, we define a ‘‘corrected’’ ft value as

$$\mathcal{F}t \equiv ft(1 + \delta_R)(1 - \delta_C) = \frac{K}{2G_V^2(1 + \Delta_R^V)} = \text{constant}, \quad (2)$$

where δ_C is the isospin-symmetry-breaking correction, δ_R is the transition-dependent part of the radiative correction, and Δ_R^V is the transition-independent part. Fortunately these corrections are all of order 1% but, even so, to maintain an accuracy criterion of 0.1% they must be calculated with an accuracy of 10% of their central value. This is a demanding request, especially for the nuclear-structure-dependent corrections.

To separate out those terms that are dependent on nuclear structure from those that are not, we split the transition-dependent radiative correction into two terms,

$$\delta_R = \delta'_R + \delta_{NS}, \quad (3)$$

of which the first, δ'_R , is a function only of the electron's energy and the charge of the daughter nucleus Z ; it therefore depends on the particular nuclear decay, but is *independent* of nuclear structure. The second term, δ_{NS} , like δ_C , depends in its evaluation on the details of nuclear structure. To emphasize the different sensitivities of the correction terms, we rewrite the expression for $\mathcal{F}t$ as

$$\mathcal{F}t \equiv ft(1 + \delta'_R)(1 + \delta_{NS} - \delta_C), \quad (4)$$

where the first correction in brackets is independent of nuclear structure, while the second incorporates the structure-dependent terms.

Our procedure in this paper will be to examine all experimental data related to 20 super-allowed transitions, comprising those that have been well studied, together with others that have only recently become accessible to precision measurement. The methods used and the data accepted are presented in Sect. II. The calculations and corrections required to extract final $\mathcal{F}t$ -values from these data are described and applied in Sect. III; in the same section, we use the resulting $\mathcal{F}t$ -values to test CVC. Finally, in Sect. IV we explore the impact of these results on a number of weak-interaction issues: CKM unitarity as well as the possible existence of scalar or right-hand currents.

II. EXPERIMENTAL DATA

The ft -value that characterizes any β -transition depends on three measured quantities: the total transition energy, Q_{EC} , the half-life, $t_{1/2}$, of the parent state and the branching ratio, R , for the particular transition of interest. The Q_{EC} -value is required to determine

the statistical rate function, f , while the half-life and branching ratio combine to yield the partial half-life, t . In tables I-VII we present the measured values of these three quantities and supporting information for a total of twenty superallowed transitions, incorporating the eight cases we dealt with in our last complete survey [6], but now including four more cases that have been measured more recently with comparable precision, and a further eight that are likely to become accessible to precision measurements within the next few years.

A. Evaluation principles

In our treatment of the data, we considered all measurements formally published before November 2004 and those we knew to be in an advanced state of preparation for publication by that date. We scrutinized all the original experimental reports in detail. Where necessary and possible, we used the information provided there to correct the results for calibration data that have improved since the measurement was made. If corrections were evidently required but insufficient information was provided to make them, the results were rejected. Of the surviving results, only those with (updated) uncertainties that are within a factor of ten of the most precise measurement for each quantity were retained for averaging in the tables. Each datum appearing in the tables is attributed to its original journal reference *via* an alphanumeric code comprising the initial two letters of the first author’s name and the two last digits of the publication date. These alphanumeric codes are correlated with the actual reference numbers in Table VIII.

The statistical procedures we have followed in analyzing the tabulated data are based on those used by the Particle Data Group in their periodic reviews of particle properties, e.g. ref [7], and adopted by us in earlier surveys [4, 6] of superallowed $0^+ \rightarrow 0^+$ beta decay. In the tables and throughout this work, “error bars” and “uncertainties” always refer to plus-and-minus one standard deviation (68% confidence level). For a set of N uncoupled measurements, $x_i \pm \delta x_i$, of a particular quantity, a gaussian distribution is assumed, the weighted average being calculated according to:

$$\bar{x} \pm \delta\bar{x} = \frac{\sum_i w_i x_i}{\sum_i w_i} \pm (\sum_i w_i)^{-1/2}, \quad (5)$$

where

$$w_i = 1/(\delta x_i)^2$$

and the sums extend over all N measurements. For each average, the χ^2 is also calculated and a scale factor, S , determined:

$$S = \left[\chi^2 / (N - 1) \right]^{1/2}. \quad (6)$$

This factor is then used to establish the quoted uncertainty. If $S \leq 1$, the value of $\delta\bar{x}$ from Eq. (5) is left unchanged. If $S > 1$ and the input δx_i are all about the same size, then we increase $\delta\bar{x}$ by the factor S , which is equivalent to assuming that all the experimental errors were underestimated by the same factor. Finally, if $S > 1$ but the δx_i are of widely varying magnitudes, S is recalculated with only those results for which $\delta x_i \leq 3N^{1/2}\delta\bar{x}$ being retained; the recalculated scale factor is then applied in the usual way. In all three cases, no change is made to the original average \bar{x} calculated with Eq. (5).

The data for Q_{EC} include measurements of both individual Q_{EC} -values and the differences between pairs of Q_{EC} -values. This required a two-step analysis procedure. We first treated the individual Q_{EC} -value measurements for each particular transition in the manner already described, obtaining an average result with uncertainty in each case, $\tilde{x}_j \pm \delta\tilde{x}_j$, where the subscript j now designates a particular transition. For transitions unconnected by difference measurements, these uncertainties were scaled if necessary and then the values were quoted as final results. For those transitions involved in one or more difference measurements we combined their average Q_{EC} values, $\tilde{x}_j \pm \delta\tilde{x}_j$, with the difference measurements, $d_k \pm \delta d_k$, in a single fitting procedure. If M_1 is the number of transitions that are connected by difference measurements, and M_2 is the number of those difference measurements, then we have a total of $M_1 + M_2$ input data values from which we need to extract a final set of M_1 average Q_{EC} -values, $\bar{x}_j \pm \delta\bar{x}_j$. We accomplish this by minimizing χ^2 , where

$$\chi^2 = \sum_{j=1}^{M_1} \left(\frac{\tilde{x}_j - \bar{x}_j}{\delta\tilde{x}_j} \right)^2 + \sum_{k=1}^{M_2} \left(\frac{d_k - \bar{d}_k}{\delta d_k} \right)^2 \quad (7)$$

and

$$\bar{d}_k = \bar{x}_{j_1} - \bar{x}_{j_2},$$

with j_1 and j_2 designating the two transitions whose Q_{EC} -value difference is determined in a particular d_k measurement. For each of these individual Q_{EC} -values, we obtained its scale factor from Eq. (6), where the χ^2 used in that equation is now given by

$$\chi^2 = \sum_i \left(\frac{x_i - \bar{x}_j}{\delta x_i} \right)^2 + \sum_l \left(\frac{d_l - \bar{d}_l}{\delta d_l} \right)^2, \quad (8)$$

where j is the particular transition of interest. The sum in i extends over all individual Q_{EC} -value measurements of transition j , and the sum in l extends over all doublet measurements that include transition j as one component. The resultant value of S was applied to the uncertainty, $\delta\bar{x}_j$, with the same conventions as were described previously.

B. Data tables

The Q_{EC} -value data appear in Tables I and II. For the best-known nine superallowed decays – those of ^{10}C , ^{14}O , $^{26}\text{Al}^m$, ^{34}Cl , $^{38}\text{K}^m$, ^{42}Sc , ^{46}V , ^{50}Mn and ^{54}Co – the daughter nuclei are stable, and the most precise determinations of their Q_{EC} -values have come from direct measurements of that property *via*, for example, (p,n) or (^3He ,t) reactions. Such measurements are identified in column 3 of Table I by “ $Q_{EC}(sa)$ ” and each individual result is itemized with its appropriate reference in the next three columns. The weighted average (see Eq. (5)) of all measurements for a particular decay appears in column 7, with the corresponding scale factor (see Eq. (6)) in column 8. A few of these cases, like ^{34}Cl and ^{46}V , have no further complications. There are other cases, however, in which Q_{EC} -value differences have been measured in addition to the individual Q_{EC} -values. These measurements are presented in Table II. They have been dealt with in combination with the direct Q_{EC} -value measurements, as described in section II A (see, in particular, Eq. (7)), with the final average Q_{EC} -value appearing in column 7 of Table I and the average difference in column 4 of Table II. Both are flagged with footnotes to indicate the interconnection.

TABLE I: Decay energies, Q_{EC} , for superallowed β -decay branches. (See Table VIII for the correlation between the alphanumeric reference code used in this table and the actual reference numbers.)

Parent/Daughter		Property ¹	Measured Energy, Q_{EC} (keV)			Average value	
nuclei			1	2	3	Energy (keV)	scale
$T_z = -1$:							
^{10}C	^{10}B	$Q_{EC}(gs)$	3647.84 ± 0.34 [Ba84]	3647.95 ± 0.12 [Ba98]		3647.94 ± 0.11	1.0
		$E_x(d0^+)$	1740.15 ± 0.17 [Aj88]	1740.07 ± 0.02 ²		1740.07 ± 0.02	1.0
		$Q_{EC}(sa)$				1907.87 ± 0.11	
^{14}O	^{14}N	$Q_{EC}(gs)$	5143.35 ± 0.60 [Bu61]	5145.09 ± 0.46 [Ba62]	5145.57 ± 0.48 [Ro70]		
			5142.71 ± 0.80 [Vo77]	5143.43 ± 0.37 [Wh77]	5144.34 ± 0.17 [To03]	5144.29 ± 0.28	2.1

TABLE I (continued)

Parent/Daughter		Property ¹	Measured Energy (keV)			Average value	
nuclei			1	2	3	Energy (keV)	scale
		$E_x(d0^+)$	2312.798 ± 0.011 [Aj91]			2312.798 ± 0.011	
		$Q_{EC}(sa)$				2831.18 ± 0.24 ³ 2.5	
¹⁸ Ne	¹⁸ F	$ME(p)$	5316.8 ± 1.5 [Ma94]	5317.63 ± 0.36 [Bl04b]		5317.58 ± 0.35	1.0
		$ME(d)$	873.31 ± 0.94 [Bo64]	875.5 ± 2.2 [Ho64]	876.5 ± 2.8 [Pr67]		
			877.2 ± 3.0 [Se73]	873.96 ± 0.61 [Ro75]		874.02 ± 0.48	1.0
		$Q_{EC}(gs)$	4438 ± 9 [Fr63]			4443.54 ± 0.60	1.0
		$E_x(d0^+)$	1041.55 ± 0.08 [Ti95]			1041.55 ± 0.08	
		$Q_{EC}(sa)$				3401.99 ± 0.60	
²² Mg	²² Na	$ME(p)$	-401.3 ± 3.0 [Ha74c]	-400.5 ± 1.3 ⁴		-400.6 ± 1.2	1.0
		$ME(d)$	-5184.3 ± 1.5 [We68]	-5182.5 ± 0.5 [Be68]	-5181.3 ± 1.7 [An70]		
			-5183.2 ± 1.0 [Gi72]	-5181.56 ± 0.16 [Mu04]	-5181.08 ± 0.30 [Sa04]	-5181.58 ± 0.27	2.4
		$Q_{EC}(gs)$	4781.64 ± 0.28 [Mu04]	4781.40 ± 0.67 [Sa04]		4781.58 ± 0.25	1.0
		$E_x(d0^+)$	657.00 ± 0.14 [En98]			657.00 ± 0.14	
		$Q_{EC}(sa)$				4124.58 ± 0.29	
²⁶ Si	²⁶ Al	$ME(p)$	-7159 ± 18 [Mi67]	-7149 ± 30 [Mc67]	-7139 ± 30 [Ha68]		
			-7145.5 ± 3.0 [Ha74c]			-7145.8 ± 2.9	1.0
		$ME(d0^+)$	-11982.08 ± 0.26 ⁵			-11982.08 ± 0.26	
		$Q_{EC}(sa)$	4850 ± 13 [Fr63]			4836.9 ± 3.0	1.0
³⁰ S	³⁰ P	$ME(p)$	-14060 ± 15 [Mi67]	-14054 ± 25 [Mc67]	-14068 ± 30 [Ha68]		
			-14063.4 ± 3.0 [Ha74c]			-14063.2 ± 2.9	1.0
		$ME(d)$	-20203 ± 3 [Ha67]	-20200.58 ± 0.40 [Re85]		-20200.62 ± 0.40	1.0
		$Q_{EC}(gs)$				6137.4 ± 2.9	
		$E_x(d0^+)$	677.29 ± 0.07 [En98]			677.29 ± 0.07	
		$Q_{EC}(sa)$	5437 ± 17 [Fr63]			5459.5 ± 3.9	1.3
³⁴ Ar	³⁴ Cl	$ME(p)$	-18380.2 ± 3.0 [Ha74c]	-18377.10 ± 0.41 [He02]		-18377.17 ± 0.40	1.0
		$ME(d)$	-24440.01 ± 0.23 ⁵			-24440.01 ± 0.23	
		$Q_{EC}(sa)$				6062.83 ± 0.46	
³⁸ Ca	³⁸ K	$ME(p)$	-22056.0 ± 5.0 [Se74]			-22056.0 ± 5.0	
		$ME(d0^+)$	-28670.20 ± 0.32 ⁵			-28670.20 ± 0.32	
		$Q_{EC}(sa)$				6614.2 ± 5.0	
⁴² Ti	⁴² Sc	$ME(p)$	-25121 ± 6 [Mi67]	-25086 ± 30 [Ha68]	-25124 ± 13 [Zi72]	-25120.7 ± 5.3	1.0
		$ME(d)$	-32121.55 ± 0.80 ⁵			-32121.55 ± 0.80	
		$Q_{EC}(sa)$				7000.9 ± 5.4	
$T_z = 0:$							
²⁶ Al ^m	²⁶ Mg	$Q_{EC}(gs)$	4004.79 ± 0.55 [De69]	4004.41 ± 0.10 ⁶		4004.42 ± 0.10	1.0
		$E_x(p0^+)$	228.305 ± 0.013 [En98]			228.305 ± 0.013	

TABLE I (continued)

Parent/Daughter Property ¹		Measured Energy (keV)			Average value	
nuclei		1	2	3	Energy (keV)	scale
	$Q_{EC}(sa)$	4232.71 ± 0.60 [Vo77]	4232.19 ± 0.12 [Br94]		4232.55 ± 0.17 ³	2.7
³⁴ Cl	³⁴ S $Q_{EC}(sa)$	5490.3 ± 1.9 [Ry73a]	5491.6 ± 2.3 [Ha74d]	5491.71 ± 0.54 [Ba77c]		
		5492.2 ± 0.4 [Vo77]	5491.65 ± 0.26 ⁷		5491.78 ± 0.20	1.0
³⁸ K ^m	³⁸ Ar $Q_{EC}(gs)$	5914.76 ± 0.60 [Ja78]			5914.76 ± 0.60	
	$E_x(p0^+)$	130.4 ± 0.3 [En98]			130.4 ± 0.3	
	$Q_{EC}(sa)$	6044.6 ± 1.5 [Bu79]	6044.38 ± 0.12 [Ha98]		6044.40 ± 0.11	1.0
⁴² Sc	⁴² Ca $Q_{EC}(sa)$	6423.71 ± 0.40 [Vo77]	6425.84 ± 0.17 ⁸		6425.63 ± 0.38 ³	3.2
⁴⁶ V	⁴⁶ Ti $Q_{EC}(sa)$	7053.3 ± 1.8 [Sq76]	7050.41 ± 0.60 [Vo77]		7050.71 ± 0.89	1.6
⁵⁰ Mn	⁵⁰ Cr $Q_{EC}(sa)$	7632.8 ± 2.8 [Ha74d]	7631.91 ± 0.40 [Vo77]		7632.43 ± 0.23 ³	1.0
⁵⁴ Co	⁵⁴ Fe $Q_{EC}(sa)$	8241.2 ± 1.8 [Ho74]	8245.6 ± 3.0 [Ha74d]	8241.61 ± 0.60 [Vo77]	8242.60 ± 0.29 ³	1.5
⁶² Ga	⁶² Zn $Q_{EC}(sa)$	9171 ± 26 [Da79]			9171 ± 26	
⁶⁶ As	⁶⁶ Ge $Q_{EC}(sa)$	9550 ± 50 [Da80]			9550 ± 50	
⁷⁰ Br	⁷⁰ Se $Q_{EC}(sa)$	9970 ± 170 [Da80]			9970 ± 170	
⁷⁴ Rb	⁷⁴ Kr $ME(p)$	-51905 ± 18 [He02]	-51915.2 ± 4.0 [Ke04]		-51914.7 ± 3.9	1.0
	$ME(d)$	-62330.3 ± 2.4 [He02]	-62332.0 ± 2.1 [Ke04]		-62331.3 ± 1.6	1.0
	$Q_{EC}(sa)$				10416.5 ± 4.2	

¹ Abbreviations used in this column are as follows: “*gs*”, transition between ground states; “*sa*”, super-allowed transition; “*p*”, parent; “*d*”, daughter; “*ME*”, mass excess; “ $E_x(0^+)$ ”, excitation energy of the 0^+ (analog) state. Thus, for example, “ $Q_{EC}(sa)$ ” signifies the Q_{EC} -value for the superallowed transition, “ $ME(d)$ ”, the mass excess of the daughter nucleus; and “ $ME(d0^+)$ ”, the mass excess of the daughter’s 0^+ state.

² Result based on references [Ba88] and [Ba89].

³ Average result includes the results of Q_{EC} pairs; see Table II.

⁴ Result based on references [Bi03] and [Se04].

⁵ Result obtained from data elsewhere in this table.

⁶ Result based on references [Is80], [Al82], [Hu82], [Be85], [Pr90], [Ki91] and [Wa92].

⁷ Result based on references [Wa83], [Ra83] and [Li94].

⁸ Result based on references [Zi87] and [Ki89].

TABLE II: Q_{EC} -value differences for superallowed β -decay branches. These data are also used as input to determine some of the average Q_{EC} -values listed in Table I. (See Table VIII for the correlation between the alphabetical reference code used in this table and the actual reference numbers.)

Parent	Parent	$Q_{EC2} - Q_{EC1}$ (keV)	
nucleus 1	nucleus 2	measurement	average ^a
¹⁴ O	²⁶ Al ^m	1401.68 ± 0.13 [Ko87]	1401.37 ± 0.29
²⁶ Al ^m	⁴² Sc	2193.5 ± 0.2 [Ko87]	2193.09 ± 0.42
⁴² Sc	⁵⁰ Mn	1207.6 ± 2.3 [Ha74d]	1206.79 ± 0.44
⁴² Sc	⁵⁴ Co	1817.2 ± 0.2 [Ko87]	1816.97 ± 0.48
⁵⁰ Mn	⁵⁴ Co	610.09 ± 0.17 ^[Ko87] _[Ko97b]	610.18 ± 0.37

^aAverage values include the results of direct Q_{EC} -value measurements: see Table I.

There are two cases, ²⁶Al^m and ³⁸K^m, in which the superallowed decay originates from an isomeric state. For both, there are Q_{EC} -value measurements that correspond to the ground state as well as to the isomer. Obviously, these two sets of measurements are simply related to one another by the excitation energy of the isomeric state in the parent. In Table I, the set of measurements for the ground-state Q_{EC} -value and for the excitation energy of the isomeric state appear in separate rows, each with its identifying property given in column 3 and its weighted average appearing in column 7. In the row below, the average value given in column 7 for the superallowed transition is the weighted average not only of the direct superallowed Q_{EC} -value measurements in that row, but also of the result derived from the two preceding rows. Note that in all cases the Q_{EC} -value for the superallowed transition appears in bold-face type.

For those 11 superallowed decays that lead to radioactive daughter nuclei, there are very few direct measurements of the Q_{EC} -value for the superallowed transition. In general, that Q_{EC} -value must be deduced from the measured mass excesses of the parent and daughter nuclei, together with the excitation energy of the analog 0⁺ state in the daughter. Each of these properties is identified in column 3 of Table I, with the individual measurements of that property, their weighted average and a scale factor appearing in columns to the right.

TABLE III: Half-lives, $t_{1/2}$, of superallowed β -emitters. (See Table VIII for the correlation between the alphabetical reference code used in this table and the actual reference numbers.)

Parent nucleus	Measured half-lives, $t_{1/2}$ (ms)				Average value	
	1	2	3	4	$t_{1/2}$ (ms)	scale
$T_z = -1$:						
^{10}C	19280 \pm 20 [Az74]	19295 \pm 15 [Ba90]			19290 \pm 12	1.0
^{14}O	70480 \pm 150 [Al72]	70588 \pm 28 [Cl73]	70430 \pm 180 [Az74]	70684 \pm 77 [Be78]		
	70613 \pm 25 [Wi78]	70560 \pm 49 [Ga01]	70641 \pm 20 [Ba04]		70616 \pm 14	1.1
^{18}Ne	1690 \pm 40 [As70]	1670 \pm 20 [Al70]	1669 \pm 4 [Al75]	1687 \pm 9 [Ha75]	1672.1 \pm 4.6	1.3
^{22}Mg	3857 \pm 9 [Ha75]	3875.5 \pm 1.2 [Ha03]			3875.2 \pm 2.4	2.0
^{26}Si	2210 \pm 21 [Ha75]	2240 \pm 10 [Wi80]			2234 \pm 12	1.3
^{30}S	1180 \pm 40 [Ba67]	1220 \pm 30 [Mo71]	1178.3 \pm 4.8 [Wi80]		1179.4 \pm 4.7	1.0
^{34}Ar	844.5 \pm 3.4 [Ha74a]	847.0 \pm 3.7 [Ia03]			845.6 \pm 2.5	1.0
^{38}Ca	470 \pm 20 [Ka68]	439 \pm 12 [Ga69]	450 \pm 70 [Zi72]	430 \pm 12 [Wi80]	440.0 \pm 7.8	1.2
^{42}Ti	200 \pm 20 [Ni69]	202 \pm 5 [Ga69]	173 \pm 14 [Al69]		198.8 \pm 6.3	1.4
$T_z = 0$:						
$^{26}\text{Al}^m$	6346 \pm 5 [Fr69a]	6346 \pm 5 [Az75]	6339.5 \pm 4.5 [Al77]	6346.2 \pm 2.6 [Ko83]	6345.0 \pm 1.9	1.0
	6345 \pm 14 [Sc05]					
^{34}Cl	1526 \pm 2 [Ry73a]	1525.2 \pm 1.1 [Wi76]	1527.7 \pm 2.2 [Ko83]	1527.1 \pm 0.5 [Ia03]	1526.77 \pm 0.44	1.0
$^{38}\text{K}^m$	925.6 \pm 0.7 [Sq75]	922.3 \pm 1.1 [Wi76]	921.71 \pm 0.65 [Wi78]	924.15 \pm 0.31 [Ko83]		
	924.4 \pm 0.6 [Ba00]	924.46 \pm 0.14 [Ba05]			924.33 \pm 0.27	2.3
^{42}Sc	680.98 \pm 0.62 [Wi76]	680.67 \pm 0.28 [Ko97a]			680.72 \pm 0.26	1.0
^{46}V	422.47 \pm 0.39 [Al77]	422.28 \pm 0.23 [Ba77a]	422.57 \pm 0.13 [Ko97a]		422.50 \pm 0.11	1.0
^{50}Mn	284.0 \pm 0.4 [Ha74b]	282.8 \pm 0.3 [Fr75]	282.72 \pm 0.26 [Wi76]	283.29 \pm 0.08 [Ko97a]	283.24 \pm 0.13	1.8
^{54}Co	193.4 \pm 0.4 [Ha74b]	193.0 \pm 0.3 [Ho74]	193.28 \pm 0.18 [Al77]	193.28 \pm 0.07 [Ko97a]	193.271 \pm 0.063	1.0
^{62}Ga	115.95 \pm 0.30 [Al78]	116.34 \pm 0.35 [Da79]	115.84 \pm 0.25 [Hy03]	116.19 \pm 0.04 [Bl04a]	116.175 \pm 0.038	1.0
	116.09 \pm 0.17 [Ca05]					
^{66}As	95.78 \pm 0.39 [Al78]	95.77 \pm 0.28 [Bu88]			95.77 \pm 0.23	1.0
^{70}Br	80.2 \pm 0.8 [Al78]	78.54 \pm 0.59 [Bu88]			79.12 \pm 0.79	1.7
^{74}Rb	64.90 \pm 0.09 [Oi01]	64.761 \pm 0.031 [Ba01]			64.776 \pm 0.043	1.5

The average Q_{EC} -value listed for the corresponding superallowed transition is obtained from these separate averages. If a direct measurement of the superallowed Q_{EC} -value exists, then it is also included in the final average.

Especially in these latter 11 cases, it might be imagined that it would have been sufficient for us to use the 2003 Mass tables [20] to derive the Q_{EC} -values of interest. There are, however, significant differences in our approach. We have included all pertinent measurements for each property as described in section II A; typically, only a subset of the available data is included as input to the mass tables. Furthermore, we have examined each reference in detail and either accepted the result, updated it to modern calibration standards or rejected

TABLE IV: Branching ratios, R, for superallowed β -transitions. (See Table VIII for the correlation between the alphabetical reference code used in this table and the actual reference numbers.)

Parent/Daughter nuclei	Daughter state E_x (MeV)	Measured Branching Ratio, R (%)		Average value		
		1	2	R (%)	scale	
$T_z = -1$:						
^{10}C	^{10}B	2.16	$0_{-0}^{+0.0008}$ [Go72]		$0_{-0}^{+0.0008}$	
		1.74	1.468 ± 0.014 [Ro72]	1.473 ± 0.007 [Na91]		
			1.465 ± 0.009 [Kr91]	1.4625 ± 0.0025 [Sa95]		
			1.4665 ± 0.0038 [Fu99]		1.4646 ± 0.0019	1.0
^{14}O	^{14}N	gs	0.60 ± 0.10 [Sh55]	0.65 ± 0.05 [Fr63]		
			0.61 ± 0.01 [Si66]		0.611 ± 0.010	1.0
		3.95	0.062 ± 0.007 [Ka69]	0.058 ± 0.004 [Wi80]		
			0.053 ± 0.002 [He81]		0.0545 ± 0.0019	1.1
		2.31			99.334 ± 0.010	
^{18}Ne	^{18}F	1.04	9 ± 3 [Fr63]	7.70 ± 0.21^a [Ha75]	7.70 ± 0.21	1.0
^{22}Mg	^{22}Na	0.66	54.0 ± 1.1 [Ha75]	53.15 ± 0.12 [Ha03]	53.16 ± 0.12	1.0
^{26}Si	^{26}Al	1.06	21.8 ± 0.8 [Ha75]		21.8 ± 0.8	
		0.23			75.09 ± 0.92^a	
^{30}S	^{30}P	gs	20 ± 1 [Fr63]		20 ± 1	
		0.68			77.4 ± 1.0^a	
^{34}Ar	^{34}Cl	0.67	2.49 ± 0.10 [Ha74a]		2.49 ± 0.10	
		gs			94.45 ± 0.25^a	
^{42}Ti	^{42}Sc	0.61	56 ± 14 [Al69]		56 ± 14	
		gs			43 ± 14^a	
$T_z = 0$:						
$^{26}\text{Al}^m$	^{26}Mg	gs	>99.997 [Ki91]		$100.000_{-0.003}^{+0}$	
^{34}Cl	^{34}S	gs	>99.988 [Dr75]		$100.000_{-0.012}^{+0}$	
$^{38}\text{K}^m$	^{38}Ar	3.38	<0.0019 [Ha94]		$0_{-0}^{+0.002}$	
		gs	>99.998		$100.000_{-0.002}^{+0}$	
^{42}Sc	^{42}Ca	1.84	0.0063 ± 0.0026 [In77]	0.0022 ± 0.0017 [De78]		
			0.0103 ± 0.0031 [Sa80]	0.0070 ± 0.0012 [Da85]	0.0059 ± 0.0014	1.6
		gs			99.9941 ± 0.0014	
^{46}V	^{46}Ti	2.61	0.0039 ± 0.0004 [Ha94]		0.0039 ± 0.0004	
		4.32	0.0113 ± 0.0012 [Ha94]		0.0113 ± 0.0012	
		ΣGT^b	<0.004		$0_{-0}^{+0.004}$	
	gs			$99.9848_{-0.0042}^{+0.0013}$		
^{50}Mn	^{50}Cr	3.63	0.057 ± 0.003 [Ha94]		0.057 ± 0.003	
		3.85	<0.0003 [Ha94]		$0_{-0}^{+0.0003}$	
		5.00	0.0007 ± 0.0001 [Ha94]		0.0007 ± 0.0001	
	gs			99.9423 ± 0.0030		
^{54}Co	^{54}Fe	2.56	0.0045 ± 0.0006 [Ha94]		0.0045 ± 0.0006	
		ΣGT^b	<0.03		$0_{-0}^{+0.03}$	
		gs			$99.9955_{-0.0300}^{+0.0006}$	
^{62}Ga	^{62}Zn	ΣGT^b	$0.15_{-0.05}^{+0.15}$ [Hy03],[Bl02]		$0.15_{-0.05}^{+0.15}$	
	gs			$99.85_{-0.15}^{+0.05}$		
^{74}Rb	^{74}Kr	ΣGT^b	0.50 ± 0.10 [Pi03]		0.50 ± 0.10	
		gs			99.50 ± 0.10	

^aResult also incorporates data from Table V

^bdesignates total Gamow-Teller transitions to levels not explicitly listed; values were derived with the help of calculations in [Ha02].

TABLE V: Relative intensities of β -delayed γ -rays in the superallowed β -decay daughters. These data are used to determine some of the branching ratios presented in Table IV. (See Table VIII for the correlation between the alphabetical reference code used in this table and the actual reference numbers.)

Parent/Daughter		daughter ratios ^a	Measured γ -ray Ratio				Average value				
nuclei			1		2		Ratio	scale			
¹⁸ Ne	¹⁸ F	$\gamma_{660}/\gamma_{1042}$	0.021 ± 0.003	[Ha75]	0.0169 ± 0.0004	[He82]	0.0171 ± 0.0003	1.0			
			0.0172 ± 0.0005	[Ad83]							
²⁶ Si	²⁶ Al	$\gamma_{1622}/\gamma_{829}$	0.149 ± 0.016	[Mo71]	0.134 ± 0.005	[Ha75]	0.1265 ± 0.0036	1.7			
			0.1245 ± 0.0023	[Wi80]							
			0.00145 ± 0.00032	[Wi80]			0.0015 ± 0.0003				
			0.013 ± 0.003	[Mo71]		0.016 ± 0.003	[Ha75]				
			0.01179 ± 0.00027	[Wi80]				0.0118 ± 0.0003	1.0		
			0.00282 ± 0.00010	[Wi80]			0.0028 ± 0.0001				
$\gamma_{\text{total}}/\gamma_{829}$			0.1426 ± 0.0036								
³⁰ S	³⁰ P	$\gamma_{709}/\gamma_{677}$	0.006 ± 0.003	[Mo71]	0.0037 ± 0.0009	[Wi80]	0.0039 ± 0.0009	1.0			
			0.033 ± 0.002	[Mo71]		0.0290 ± 0.0006			[Wi80]	0.0293 ± 0.0011	1.9
			0.00013 ± 0.00006	[Wi80]					0.0001 ± 0.0001		
			$\gamma_{\text{total}}/\gamma_{677}$						0.0334 ± 0.0014		
³⁴ Ar	³⁴ S	$\gamma_{461}/\gamma_{666}$	0.28 ± 0.16	[Mo71]	0.365 ± 0.036	[Ha74a]	0.361 ± 0.035	1.0			
			0.38 ± 0.09	[Mo71]		0.345 ± 0.01			[Ha74a]	0.345 ± 0.010	1.0
			0.67 ± 0.08	[Mo71]		0.521 ± 0.012			[Ha74a]	0.524 ± 0.022	1.8
			$\gamma_{\text{total}}/\gamma_{666}$						1.231 ± 0.043		
⁴² Ti	⁴² Sc	$\gamma_{2223}/\gamma_{611}$	0.012 ± 0.004	[Ga69]			0.012 ± 0.004				
			2×0.012	[En90]			0.024 ± 0.008				

^a γ -ray intensities are denoted by γ_E , where E is the γ -ray energy in keV.

it for cause. The updating procedures are outlined, reference by reference, in Table VI and the rejected results are similarly documented in Table VII. With a comparatively small data set, we could afford to pay the kind of individual attention that is impossible when one is considering all nuclear masses.

The half-life data appear in Table III in similar format to Table I. For obvious reasons, half-life measurements do not lend themselves to being updated. Consequently, a number of mostly pre-1970 measurements have been rejected because they were not analyzed with the “maximum-likelihood” method. The importance of using this technique for precision measurements was not recognized until that time [64] and, without access to the primary data, there is no way a new analysis can be applied retroactively. All rejected half-life

TABLE VI: References for which the original decay-energy results have been updated to incorporate the most recent calibration standards. (See Table VIII for the correlation between the alphabetical reference code used in this table and the actual reference numbers.)

References (parent nucleus) ^a	Update procedure
<ul style="list-style-type: none"> • Bo64 (¹⁸Ne), Ba84 (¹⁰C), Br94 (²⁶Al^m) 	<ul style="list-style-type: none"> • We have converted all original (p,n) threshold measurements to Q-values using the most recent mass excesses [Au03].
<ul style="list-style-type: none"> • Ba98 (¹⁰C), Ha98 (³⁸K^m), To03 (¹⁴O) 	<ul style="list-style-type: none"> • These (p,n) threshold measurements have been adjusted to reflect recent calibration α-energies [Ry91] before being converted to Q-values.
<ul style="list-style-type: none"> • Ry73a (³⁴Cl), Ho74 (⁵⁴Co), Sq76 (⁴⁶V) 	<ul style="list-style-type: none"> • Before conversion to a Q-value, this (p,n) threshold was adjusted to reflect a new value for the ⁷Li(p,n) threshold [Wh85], which was used as calibration.
<ul style="list-style-type: none"> • Ba77c (³⁴Cl), Wh77 (¹⁴O) 	<ul style="list-style-type: none"> • This (p,n) threshold was measured relative to those for ¹⁰C and ¹⁴O; we have adjusted it based on average Q-values obtained for those decays in this work.
<ul style="list-style-type: none"> • Pr67 (¹⁸Ne) 	<ul style="list-style-type: none"> • Before conversion to a Q-value, this (p,n) threshold was adjusted to reflect the modern value for the ³⁵Cl(p,n) threshold [Au03], which was used as calibration.
<ul style="list-style-type: none"> • Ja78 (³⁸K^m) 	<ul style="list-style-type: none"> • These ¹²C(³He,n) threshold measurements have been adjusted for updated calibration reactions based on current mass excesses [Au03].
<ul style="list-style-type: none"> • Bu79 (³⁸K^m) 	<ul style="list-style-type: none"> • These (³He,t) reaction Q-values were calibrated by the ²⁷Al(³He,t) reaction to excited states in ²⁷Si; they have been revised according to modern mass excesses [Au03] and excited-state energies [En98].
<ul style="list-style-type: none"> • Bu61 (¹⁴O), Ba62 (¹⁴O) 	<ul style="list-style-type: none"> • This ⁴¹Ca(p,γ) reaction Q-value was measured relative to that for ⁴⁰Ca(p,γ); we have slightly revised the result based on modern mass excesses [Au03].
<ul style="list-style-type: none"> • Ha74d (³⁴Cl, ⁵⁰Mn, ⁵⁴Co) 	<ul style="list-style-type: none"> • These (p,t) reaction Q-values have been adjusted to reflect the current Q-value for the ¹⁶O(p,t) reaction [Au03], against which they were calibrated.
<ul style="list-style-type: none"> • Ki89 (⁴²Sc) 	
<ul style="list-style-type: none"> • Ha74c (²²Mg, ²⁶Si, ³⁰S, ³⁴Ar), Se74 (³⁸Ca) 	

^aThese references all appear in Table I under the appropriate parent nucleus.

measurements are also documented in Table VII.

Finally, the branching-ratio measurements are presented in Table IV. The decays of the $T_z = 0$ parents are the most straightforward since, in all these cases, the superallowed branch accounts for >99.5% of the total decay strength. Thus, even imprecise measurements of the weak non-superallowed branches can be subtracted from 100% to yield the superallowed branching ratio with good precision. For the higher- Z parents of this type, particularly ⁶²Ga and heavier, it has been shown theoretically [81] and experimentally [90, 117] that numerous very-weak Gamow-Teller transitions occur, which, in total, can carry significant decay strength. Where such unobserved transitions are expected to exist, we have used a combination of experiment and theory to account for the unobserved strength, with uncertainties being adjusted accordingly.

TABLE VII: References from which some or all results have been rejected. (See Table VIII for the correlation between the alphabetical reference code used in this table and the actual reference numbers.)

References (parent nucleus)	Reason for rejection
1. Decay-energies:	
• Pa72 (^{30}S , ^{38}Ca)	• No calibration is given for the measured (p,t) reaction Q -values; update is clearly required but none is possible.
• No74 (^{22}Mg)	• Calibration reaction Q -values have changed but calibration process is too complex to update.
• Ro74 (^{10}C)	• P.H. Barker (co-author) later considered that inadequate attention had been paid to target surface purity [Ba84].
• Ba77b (^{10}C)	• P.H. Barker (co-author) later stated [Ba84] that the (p,t) reaction Q -value could not be updated to incorporate modern calibration standards.
• Wh81 and Ba98 (^{14}O)	• The result in [Wh81] was updated in [Ba98] but then eventually withdrawn by P.H. Barker (co-author) in [To03].
2. Half-lives:	
• Ja60 ($^{26}\text{Al}^m$), He61 (^{14}O), Ba62 (^{14}O), Ea62 (^{10}C), Ba63 (^{10}C), Fr63 (^{14}O , ^{26}Si), Fr65b (^{42}Sc , ^{46}V , ^{50}Mn), Si72 (^{14}O)	• Quoted uncertainties are too small, and results likely biased, in light of statistical difficulties more recently understood (see [Fr69a]). In particular, “maximum-likelihood” analysis was not used.
• Ha72a ($^{26}\text{Al}^m$, ^{34}Cl , $^{38}\text{K}^m$, ^{42}Sc)	• All four quoted half-lives are systematically higher than more recent and accurate measurements.
• Ro74 (^{10}C)	• P.H. Barker (co-author) later considered that pile-up had been inadequately accounted for [Ba90].
• Ch84 ($^{38}\text{K}^m$)	• “Maximum-likelihood” analysis was not used.
3. Branching-ratios:	
• Fr63 (^{26}S)	• Numerous impurities present; result is obviously wrong.

The branching ratios for decays from $T_z = -1$ parents are much more challenging to determine, since the superallowed branch is usually one of several strong branches – with the notable exception of ^{14}O – and, in two of the measured cases, it actually has a branching ratio of less than 10%. The decays of ^{18}F , ^{26}Si , ^{30}S , ^{34}Ar and ^{42}Ti required special treatment in our presentation. In each of these five cases, the absolute branching ratio for a single β -transition has been measured. The branching ratios for other β -transitions must then be determined from the relative intensities of β -delayed γ -rays in the daughter. The relevant γ -ray intensity measurements appear in Table V, with their averages then being used to determine the superallowed branching-ratio averages shown in bold type in Table IV. These

TABLE VIII: Reference key, relating alphabetical reference codes used in Tables I-III to the actual reference numbers.

Table code	Reference number	Table code	Reference number	Table code	Reference number	Table code	Reference number	Table code	Reference number	Table code	Reference number
Ad83	[8]	Ba98	[33]	Dr75	[58]	He61	[83]	Mc67	[108]	Se74	[133]
Aj88	[9]	Ba00	[34]	Ea62	[59]	He81	[84]	Mi67	[109]	Se04	[134]
Aj91	[10]	Ba01	[35]	En90	[60]	He82	[85]	Mo71	[110]	Sh55	[135]
Al69	[11]	Ba04	[36]	En98	[61]	He02	[86]	Mu04	[111]	Si66	[136]
Al70	[12]	Ba05	[37]	Fr63	[62]	Ho64	[87]	Na91	[112]	Si72	[137]
Al72	[13]	Be68	[38]	Fr65b	[63]	Ho74	[88]	Ni69	[113]	Sq75	[138]
Al75	[14]	Be78	[39]	Fr69a	[64]	Hu82	[89]	No74	[114]	Sq76	[139]
Al77	[15]	Be85	[40]	Fr75	[65]	Hy03	[90]	Oi01	[115]	Ti95	[140]
Al78	[16]	Bi03	[41]	Fu99	[66]	Ia03	[91]	Pa72	[116]	To03	[141]
Al82	[17]	Bl02	[42]	Ga69	[67]	In77	[92]	Pi03	[117]	Vo77	[142]
An70	[18]	Bl04a	[43]	Ga01	[68]	Is80	[93]	Pr67	[118]	Wa83	[143]
As70	[19]	Bl04b	[44]	Go72	[70]	Ja60	[94]	Pr90	[119]	Wa92	[144]
Au03	[20]	Bo64	[45]	Gi72	[69]	Ja78	[95]	Ra83	[120]	We68	[145]
Az74	[21]	Br94	[46]	Ha67	[71]	Ka68	[96]	Re85	[121]	Wh77	[146]
Az75	[22]	Bu61	[47]	Ha68	[72]	Ka69	[97]	Ro70	[122]	Wh81	[147]
Ba62	[23]	Bu79	[48]	Ha72a	[73]	Ke04	[98]	Ro72	[123]	Wh85	[148]
Ba63	[24]	Bu88	[49]	Ha74a	[74]	Ki89	[99]	Ro74	[124]	Wi76	[149]
Ba67	[25]	Ca05	[50]	Ha74b	[75]	Ki91	[100]	Ro75	[125]	Wi78	[150]
Ba77a	[26]	Ch84	[51]	Ha74c	[76]	Ko83	[101]	Ry73a	[126]	Wi80	[151]
Ba77b	[27]	Cl73	[52]	Ha74d	[77]	Ko87	[102]	Ry91	[127]	Zi72	[152]
Ba77c	[28]	Da79	[53]	Ha75	[78]	Ko97a	[103]	Sa80	[128]	Zi87	[153]
Ba84	[29]	Da80	[54]	Ha94	[79]	Ko97b	[104]	Sa95	[129]		
Ba88	[30]	Da85	[55]	Ha98	[80]	Kr91	[105]	Sa04	[130]		
Ba89	[31]	De69	[56]	Ha02	[81]	Li94	[106]	Sc05	[131]		
Ba90	[32]	De78	[57]	Ha03	[82]	Ma94	[107]	Se73	[132]		

cases are also flagged with a table footnote.

III. THE $\mathcal{F}t$ VALUES

Having surveyed the primary experimental data, we now turn to producing a set of ft -values for the twenty superallowed transitions being considered. The statistical rate function, f , for each transition depends primarily on the charge of the daughter nucleus, Z , and on the Q_{EC} -value to the fifth power. Consequently the uncertainty in the value of f due to the experimental uncertainty in Q_{EC} is given by $(\Delta f/f) \approx 5(\Delta Q_{EC}/Q_{EC})$. Our goal in computing f therefore is to ensure that the computation itself yields percentage errors much

TABLE IX: Derived results for superallowed Fermi beta decays.

Parent nucleus	f	P_{EC} (%)	Partial half-life $t(ms)$	$ft(s)$	δ'_R (%)	$\delta_C - \delta_{NS}$ (%)	$\mathcal{F}t(s)$
$T_z = -1:$							
^{10}C	2.3009 ± 0.0012	0.297	1321000 ± 1900	3039.5 ± 4.7	1.652 ± 0.004	0.540 ± 0.039	3073.0 ± 4.9
^{14}O	42.772 ± 0.024	0.088	71151 ± 16	3043.3 ± 1.9	1.520 ± 0.008	0.570 ± 0.056	3071.9 ± 2.6
^{18}Ne	134.48 ± 0.15	0.081	21730 ± 590	2922 ± 80	1.484 ± 0.012	0.910 ± 0.047	2938 ± 80
^{22}Mg	418.44 ± 0.18	0.069	7295 ± 17	3052.4 ± 7.2	1.446 ± 0.017	0.505 ± 0.024	3080.9 ± 7.4
^{26}Si	1023.3 ± 3.7	0.064	2978 ± 40	3047 ± 42	1.420 ± 0.023	0.600 ± 0.024	3072 ± 42
^{30}S	1967.1 ± 7.8	0.066	1524 ± 21	2998 ± 44	1.405 ± 0.029	1.125 ± 0.039	3006 ± 44
^{34}Ar	3414.2 ± 1.5	0.069	896.0 ± 3.5	3059 ± 12	1.394 ± 0.035	0.825 ± 0.044	3076 ± 12
^{38}Ca	5338 ± 22	0.075			1.397 ± 0.042	0.910 ± 0.053	
^{42}Ti	7043 ± 30	0.088	470 ± 160	3300 ± 1100	1.412 ± 0.050	1.015 ± 0.110	3300 ± 1100
$T_z = 0:$							
$^{26}\text{Al}^m$	478.20 ± 0.11	0.082	6350.2 ± 1.9	3036.7 ± 1.2	1.458 ± 0.020	0.261 ± 0.024	3072.9 ± 1.5
^{34}Cl	1996.39 ± 0.41	0.080	$1527.99^{+0.44}_{-0.47}$	3050.5 ± 1.1	1.425 ± 0.032	0.720 ± 0.039	3071.7 ± 1.9
$^{38}\text{K}^m$	3298.10 ± 0.33	0.085	925.11 ± 0.27	3051.1 ± 1.0	1.423 ± 0.039	0.720 ± 0.047	3072.2 ± 2.1
^{42}Sc	4470.03 ± 1.46	0.099	681.43 ± 0.26	3046.0 ± 1.5	1.437 ± 0.047	0.460 ± 0.047	3075.6 ± 2.5
^{46}V	7200.0 ± 5.0	0.101	422.99 ± 0.11	3045.5 ± 2.2	1.429 ± 0.054	0.465 ± 0.033	3074.7 ± 3.0
^{50}Mn	10731.2 ± 1.8	0.107	283.71 ± 0.13	3044.5 ± 1.5	1.429 ± 0.062	0.547 ± 0.037	3071.1 ± 2.7
^{54}Co	15749.3 ± 3.0	0.111	$193.495^{+0.063}_{-0.086}$	$3047.4^{+1.2}_{-1.5}$	1.428 ± 0.071	0.639 ± 0.043	3071.2 ± 2.8
^{62}Ga	26250 ± 400	0.137	$116.509^{+0.070}_{-0.179}$	3058 ± 47	1.445 ± 0.087	1.42 ± 0.16	3058 ± 47
^{66}As	31610 ± 890	0.156			1.457 ± 0.095	1.45 ± 0.16	
^{70}Br	38600 ± 3600	0.175			1.47 ± 0.11	1.41 ± 0.20	
^{74}Rb	47280 ± 100	0.194	65.227 ± 0.078	3083.8 ± 7.5	1.49 ± 0.12	1.50 ± 0.41	3083 ± 15
Average (best 12), $\overline{\mathcal{F}t}$							3072.7 ± 0.8
χ^2/ν							0.42

less than those due to the uncertainty in the Q_{EC} -value, which can be $<0.02\%$ in the best cases. To this end we have written a new code, the details of which are given in Appendix A. Our final f -values and their uncertainties are recorded in column two of Table IX.

The partial half-life, t , for each transition is obtained from its total half-life, $t_{1/2}$, and branching ratio, R , according to the formula

$$t = \frac{t_{1/2}}{R} (1 + P_{EC}) \quad (9)$$

where P_{EC} is the calculated electron-capture fraction. The evaluation of P_{EC} is discussed

by Bambynek *et al.* [154] and is based on the equation

$$P_{EC} = \frac{1}{2}\pi \left[\sum_x \beta_x^2 (W_{EC} - |W_x|)^2 B_x \right] / f \quad (10)$$

The sum extends over all atomic subshells from which an electron can be captured. The factor β_x is the Coulomb amplitude of the appropriate bound-state electron radial wave function; W_{EC} is the Q_{EC} -value expressed in electron rest-mass units; W_x is the x -subshell binding energy also in electron rest-mass units; and B_x takes account of the effects of electron exchange and overlap. We have computed P_{EC} for the cases of interest here using our Q_{EC} -values from Table I and the values of $\beta_x^2 B_x$ and W_x from, respectively, Tables 1 and 2 of Appendix F in ref. [155]. The P_{EC} results are shown (as percentages) in column three of Table IX. Based on experimental tests of such P_{EC} calculations [154], we expect these results to be accurate to a few parts in 100; thus they do not contribute perceptibly to the overall uncertainties. Partial half-lives derived from Eq. (9), and corresponding ft values appear in columns four and five.

To obtain $\mathcal{F}t$ -values according to Eq. (4) we must now deal with the small correction terms. The term δ'_R has been calculated from standard QED, and is currently evaluated to order $Z\alpha^2$ and estimated in order $Z^2\alpha^3$ [156, 157]; its values, listed in column six of Table IX, are around 1.4% and can be considered to be very reliable. The structure-dependent terms δ_{NS} and δ_C , have also been calculated in the past but at various times over three decades and with a variety of different models. Their uncertainties are larger. This topic has been reviewed recently by Towner and Hardy [158], who presented new calculations of these corrections in which consistent model spaces and approximations have been used for both correction terms. The results of these new calculations are recorded in column seven of Table IX. Finally, the resulting $\mathcal{F}t$ -values are listed in column eight.

A. CVC test

We are now ready to test the CVC assertion that the $\mathcal{F}t$ values should be constant for all nuclear superallowed transitions of this type. The data in Table IX clearly satisfy the test; the weighted average of the 12 most-precise results (with “statistical” uncertainty only) is

$$\overline{\mathcal{F}t} = 3072.7 \pm 0.8s \quad (11)$$

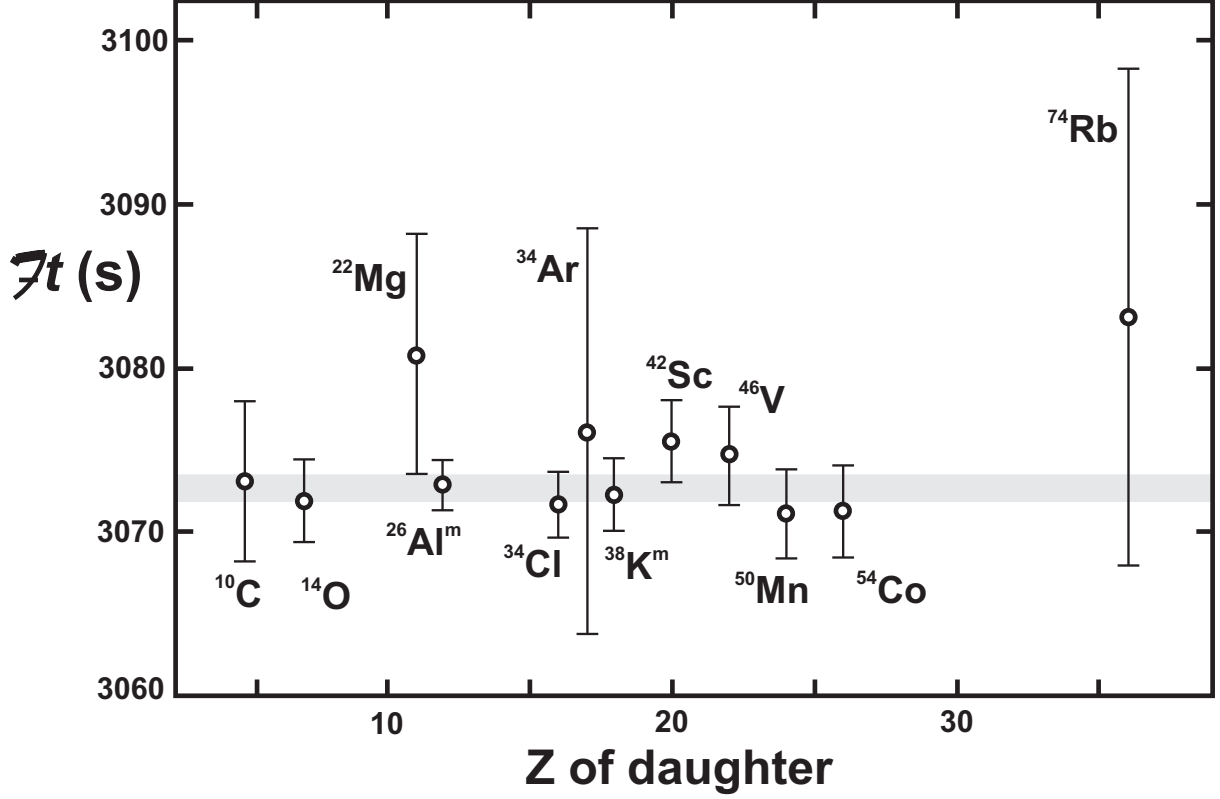


FIG. 1: $\mathcal{F}t$ values plotted as a function of the charge on the daughter nucleus, Z . The shaded horizontal band gives one standard deviation around the average $\overline{\mathcal{F}t}$ value, Eq. (11).

with a corresponding chi-square per degree of freedom of $\chi^2/\nu = 0.42$. In Fig. 1 we plot the same 12 values, all of whose statistical accuracy is better than 0.5%. It is evident from both the figure and the table that the data form a consistent set, thus verifying the expectation of the CVC hypothesis at the level of 3×10^{-4} , which is the fractional uncertainty quoted in Eq. (11). This is a 30% improvement over the results from our last survey in 1990 [6] and is principally due to improvements in the experimental data themselves.

B. $\mathcal{F}t$ -value error budgets

In Figs. 2 and 3 we show the contributing factors to the individual $\mathcal{F}t$ -value uncertainties. For the most precise data, ¹⁴O to ⁵⁴Co, which appear in Fig. 2, the theoretical uncertainties are greater than, or comparable to, the experimental ones. The nuclear-structure-dependent correction, $\delta_C - \delta_{NS}$, contributes an almost constant uncertainty of 4 parts in 10^4 across these nuclei, while the nucleus-dependent radiative correction, δ'_R , has an uncertainty that

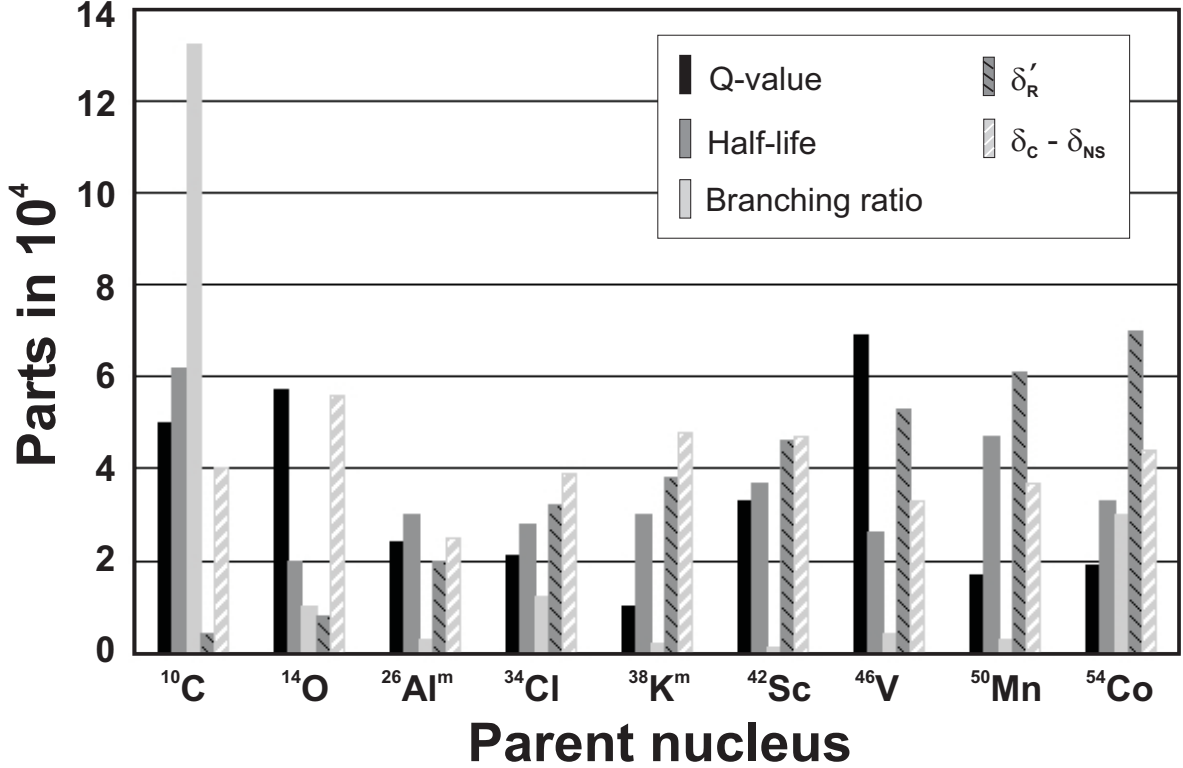


FIG. 2: Summary histogram of the fractional uncertainties attributable to each experimental and theoretical input factor that contributes to the final $\mathcal{F}t$ values for the nine most precise superallowed decay data.

grows as Z^2 . This is because the contribution to δ'_R from order $Z^2\alpha^3$ has only been estimated from its leading logarithm [156] and the magnitude of this estimate has been taken as the uncertainty in δ'_R . In fact, for ⁵⁰Mn and ⁵⁴Co this becomes the leading uncertainty, indicating that a closer look at the order $Z^2\alpha^3$ contribution would now be worthwhile. For the eight precise data, the experimental branching ratios are $> 99\%$ and have very small associated uncertainties with the exception of ⁵⁴Co, which has a 3×10^4 fractional uncertainty attributed to its branching ratio. This is because ⁵⁴Co is predicted to have several weak Gamow-Teller branches that have not yet been observed. We have used an estimate of the strength of the missing branches, taken from a shell-model calculation [81], to assign an uncertainty to the superallowed branching ratio. Missing weak branches become a larger issue for the heavier-mass nuclei with $A \geq 62$, where they contribute significantly to the branching-ratio uncertainty.

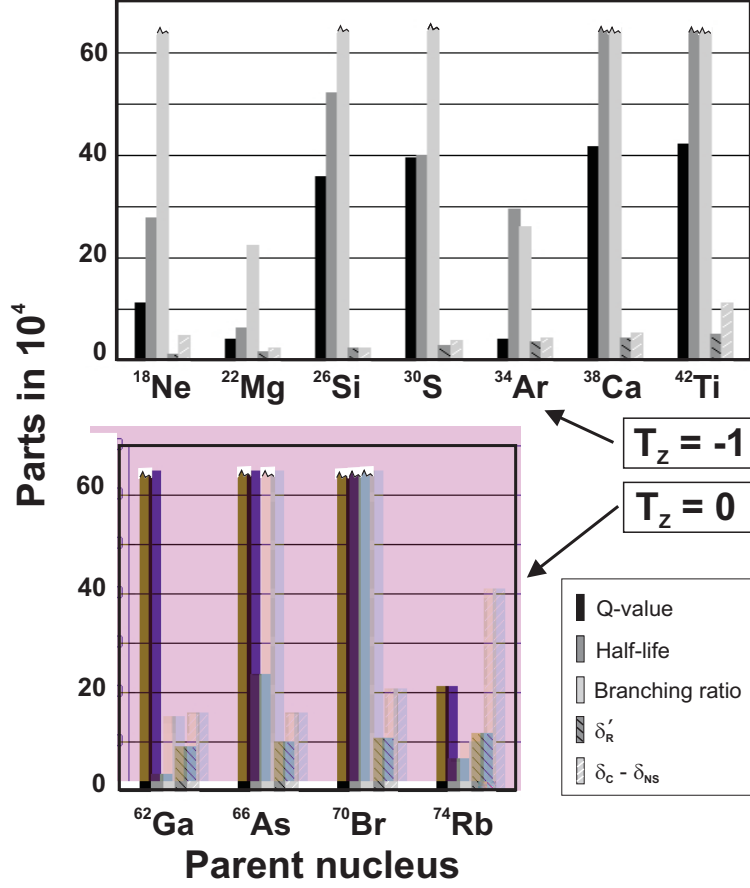


FIG. 3: Summary histogram of the fractional uncertainties attributable to each experimental and theoretical input factor that contributes to the final $\mathcal{F}t$ values for the twelve other superallowed decay data. Where the error is shown as exceeding 60 parts in 10^4 , no useful experimental measurement has been made.

For the less precisely known decay of ^{10}C , and for the twelve decays depicted in Fig. 3, the predominant uncertainties are all experimental in origin with the single exception of ^{74}Rb , for which the nuclear-structure calculation is quite difficult [158], resulting in a larger uncertainty on $\delta_C - \delta_{NS}$. Many of the experimental Q -values, half-lives and branching ratios have yet to be measured for the cases in Fig. 3, but recent advances in experimental techniques are likely to change this situation dramatically within the next few years.

C. Accounting for systematic uncertainties

So far, we have dealt with the inter-nuclear behavior of $\mathcal{F}t$ -values, examining their constancy as a test of CVC. With that test passed at high precision, we are now in a position to use the average $\mathcal{F}t$ -value obtained from these concordant nuclear data to go beyond nuclei, obtaining first the vector coupling constant (see Eq. (2)) and then the V_{ud} matrix element. Before doing so, however, we must address one more possible source of uncertainty. Though the average $\mathcal{F}t$ value given in Eq. (11) includes a full assessment of the uncertainties attributable to experiment and to the particular calculations used to obtain the correction terms, it does not incorporate any provision for a common systematic error that could arise from the type of calculation chosen to model the nuclear-structure effects. In this section we look more critically at the nuclear-structure-dependent corrections, and in particular at the isospin-symmetry-breaking correction¹, δ_C .

There have been a number of previous calculations of δ_C besides those of ours [158]: Hartree-Fock calculations of Ormand and Brown [159], RPA calculations of Sagawa, van Giai and Suzuki [160], R-matrix calculations of Barker [161], and Woods-Saxon calculations of Wilkinson [162], to name some of the more recent publications. Of these, we will only retain the Ormand-Brown (OB) calculations since they, like ours (TH), are constrained to reproduce other isospin properties of the nuclei involved: They reproduce the measured coefficients of the relevant isobaric multiplet mass equation, the known proton and neutron separation energies, and the measured ft values of weak non-analog $0^+ \rightarrow 0^+$ transitions [79], where they are known. The other calculations are not constrained by experiment in any way and thus offer no independent means to assess their efficacy.

Unfortunately, calculations of δ_C by OB are not available for all the cases listed in Table IX, so we must concentrate on the nine most precise data: ^{10}C , ^{14}O , $^{26}\text{Al}^m$, ^{34}Cl , $^{38}\text{K}^m$, ^{42}Sc , ^{46}V , ^{50}Mn , and ^{54}Co . When the TH values of δ_C are used, the average $\mathcal{F}t$ -value for these nine cases alone is $\overline{\mathcal{F}t} = 3072.6 \pm 0.8$ s with $\chi^2/\nu = 0.35$. When OB values are used for δ_C instead, the weighted average is $\overline{\mathcal{F}t} = 3074.5 \pm 0.8$ s with $\chi^2/\nu = 0.92$. Although the chi-square with the OB values is nearly a factor of three worse, we do not argue that

¹ The reason we do not consider further the nuclear-structure-dependent radiative correction, δ_{NS} , is that it is very small for the series of transitions that have $T_z = 0$ parent states [158]. Of the nine precisely known transitions we are concentrating on, seven are of this type.

this is sufficient reason to reject the OB calculation. Rather, we observe that the OB values of δ_C are systematically smaller and hence the $\mathcal{F}t$ values systematically larger than ours. Evidently there is a systematic difference between our Woods-Saxon and OB's Hartree-Fock calculations of δ_C and that difference should be accounted for in the final result. Thus, we adopt the average of these two results for our recommended $\overline{\mathcal{F}t}$, and assign a systematic uncertainty equal to half the spread between them: *viz*

$$\begin{aligned}\overline{\mathcal{F}t} &= 3073.5 \pm 0.8_{\text{stat}} \pm 0.9_{\text{syst}} \text{ s} \\ &= 3073.5 \pm 1.2 \text{ s},\end{aligned}\tag{12}$$

where the two errors have been combined in quadrature.

IV. IMPACT ON WEAK-INTERACTION PHYSICS

A. The Value of V_{ud}

With a mutually consistent set of $\mathcal{F}t$ values, we can now use their average value in Eq. (12) to determine the vector coupling constant, G_V , from Eq. (2). The value of G_V itself is of little interest, but it can be related to the weak interaction constant for the purely leptonic muon decay, G_F , to yield the much more interesting up-down matrix element of the Cabibbo-Kobayashi-Maskawa (CKM) quark-mixing matrix²: $G_V = G_F V_{ud}$. The relation we use is

$$V_{ud}^2 = \frac{K}{2G_F^2(1 + \Delta_R^V)\overline{\mathcal{F}t}},\tag{13}$$

where Δ_R^V is the nucleus-independent radiative correction. The currently accepted value for this correction is derived from the expression [163, 164]

$$\Delta_R^V = \frac{\alpha}{2\pi} [4\ln(m_Z/m_p) + \ln(m_p/m_A) + 2C_{\text{Born}}] + \dots,\tag{14}$$

where the ellipses represent further small terms of order 0.1%. Here m_Z is the Z -boson mass, m_p the proton mass, m_A the mass parameter in the dipole form of the axial-vector

² More completely we could write $G_V = G_F V_{ud} g_V(q^2 \rightarrow 0)$, where g_V is the vector form factor given in Eq. (A18), or as $G_V = G_F V_{ud} C_V$, where C_V is the vector coupling constant in the Jackson, Treiman and Wyld [165] Hamiltonian in Eq. (22), with $g_V(q^2 \rightarrow 0) = C_V = 1$.

form factor, and C_{Born} is the universal order- α axial-vector contribution. The various terms have the values

$$\Delta_{\text{R}}^{\text{V}} = 2.12 - 0.03 + 0.20 + 0.10\%, \quad (15)$$

with the first term, the leading logarithm, being essentially unambiguous in value. The final value recommended by Sirlin [164] is

$$\Delta_{\text{R}}^{\text{V}} = (2.40 \pm 0.08)\%. \quad (16)$$

The uncertainty is almost entirely due to the value selected for the axial-vector form factor mass, which Sirlin argues should lie in the range $(m_{a_1}/2) \leq m_{\text{A}} \leq 2m_{a_1}$, where m_{a_1} is the physical a_1 meson mass.

Using the Particle Data Group (PDG) [7] value for the weak interaction coupling constant from muon decay of $G_{\text{F}}/(\hbar c)^3 = (1.16639 \pm 0.00001) \times 10^{-5} \text{ GeV}^{-2}$, we obtain from Eq. (13) the result

$$|V_{ud}|^2 = 0.9482 \pm 0.0008. \quad (17)$$

Note that the total uncertainty here – 0.00083, if the next significant figure is included – is almost entirely due to the uncertainties contributed by the theoretical corrections. By far the largest contribution, 0.00074, arises from the uncertainty in $\Delta_{\text{R}}^{\text{V}}$; 0.00031 comes from the nuclear-structure-dependent corrections $\delta_{\text{C}} - \delta_{\text{NS}}$ (principally from the systematic difference between the OB and TH calculations discussed in Sect. III C) and 0.00012 is attributable to δ'_{R} . Only 0.00016 can be considered to be experimental in origin.

The corresponding value of V_{ud} is

$$|V_{ud}| = 0.9738 \pm 0.0004, \quad (18)$$

a result that differs by two units in the last quoted digit from our previously recommended result [1]. This shift, well within the quoted one standard deviation, is due to the improvements in the experimental data and to our re-computing of the statistical rate function (see Appendix A), in which a number of different parameter choices were made for the charge-density distribution, the oscillator length parameter for nuclear radial functions, and for the screening correction. Coincidentally, the value of V_{ud} quoted in Eq. (18) is identical to the currently recommended PDG value [7], although our uncertainty is one digit smaller.

B. Unitarity of the CKM matrix

The CKM matrix yields the transformation equations for a change of basis from quark weak-interaction eigenstates to quark mass eigenstates. As such, the CKM matrix must be unitary in order that the bases remain orthonormal. With the CKM matrix elements determined from experimental data, one important test they should satisfy is that they yield a unitary matrix. Currently, the sum of the squares of the top-row elements, which should equal one, constitutes the most demanding available test. With our experimental value for $|V_{ud}|^2$ given in Eq. (17) and the PDG's recommended values [7] of $|V_{us}| = 0.2200 \pm 0.0026$ and $|V_{ub}| = 0.00367 \pm 0.00047$, this unitarity test yields:

$$|V_{ud}|^2 + |V_{us}|^2 + |V_{ub}|^2 = 0.9966 \pm 0.0014 \quad (19)$$

The test fails by 2.4 standard deviations. Two-thirds of the assigned error is attributed to the uncertainty in $|V_{us}|^2$, *viz.* 0.0011, and one-third to the error in $|V_{ud}|^2$, *viz.* 0.0008. The latter, as we have already demonstrated, is *not* predominantly experimental in origin, but is dominated by the uncertainty in the nucleus-independent radiative correction, $\Delta_{\text{R}}^{\text{V}}$.

A recent measurement of the $K^+ \rightarrow \pi^0 e^+ \nu_e$ (K_{e3}^+) branching ratio from the Brookhaven E865 experiment [2] obtains $V_{us} = 0.2272 \pm 0.0030$. Although this result is included in the PDG average value, it is considerably higher than the older experimental results from K_{e3}^+ and K_{e3}^0 decays, with which it is inconsistent. Experiments now in progress should help clarify the situation. If, for the moment, we adopt the E865 value for V_{us} rather than the PDG average, then the result in Eq. (19) is modified to

$$|V_{ud}|^2 + |V_{us}|^2 + |V_{ub}|^2 = 0.9999 \pm 0.0016 \quad (20)$$

and unitarity is fully satisfied.

Another, at present, less demanding test is to examine the first column of the CKM matrix. The PDG value for V_{cd} is 0.224 ± 0.012 , but little is known about V_{td} other than it is expected to lie in the range $0.0048 \leq V_{td} \leq 0.014$. In this range it has negligible impact on the unitarity sum. With our value of $|V_{ud}|^2$, this unitarity sum becomes

$$|V_{ud}|^2 + |V_{cd}|^2 + |V_{td}|^2 = 0.9985 \pm 0.0054 \quad (21)$$

Here the error is given entirely by the uncertainty in the value of V_{cd} and unitarity is evidently satisfied at this level of accuracy.

C. Fundamental Scalar Interaction

For the past 40 years, the weak interaction has been described by an equal mix of vector and axial-vector interactions that maximizes parity violation. The theory is known colloquially as the ‘ $V - A$ ’ theory. Despite the ever increasing precision possible in weak-interaction experiments, no defect has been found in the $V - A$ theory. Prior to the establishment of the $V - A$ theory, other forms of fundamental couplings, notably scalar and tensor interactions, were popular. Today there is still interest in searching for scalar and tensor interactions, not because we expect them to contribute importantly, but rather because we wish to establish limits to their possible contribution.

A general form of the weak-interaction Hamiltonian was written down by Jackson, Treiman and Wyld [165]. In examining superallowed Fermi transitions, we are only interested in scalar and vector couplings, for which that Hamiltonian becomes

$$\begin{aligned}
 H_{S+V} = & (\bar{\psi}_p \psi_n)(C_S \bar{\phi}_e \phi_{\bar{\nu}_e} + C'_S \bar{\phi}_e \gamma_5 \phi_{\bar{\nu}_e}) \\
 & + (\bar{\psi}_p \gamma_\mu \psi_n)(C_V \bar{\phi}_e \gamma_\mu \phi_{\bar{\nu}_e} + C'_V \bar{\phi}_e \gamma_\mu \gamma_5 \phi_{\bar{\nu}_e}).
 \end{aligned}
 \tag{22}$$

If we assume that the Hamiltonian is invariant under time reversal, then all the coupling constants must be real. Those coupling constants carrying a prime represent parity-nonconserving interactions. If we further assume that parity violation is maximal, then $C'_i = C_i$. In this limit, the scalar and vector terms can be written

$$\begin{aligned}
 H_{S+V} = & (\bar{\psi}_p C_S \psi_n) (\bar{\phi}_e (1 + \gamma_5) \phi_{\bar{\nu}_e}) \\
 & + (\bar{\psi}_p C_V \gamma_\mu \psi_n) (\bar{\phi}_e \gamma_\mu (1 + \gamma_5) \phi_{\bar{\nu}_e}).
 \end{aligned}
 \tag{23}$$

A nonrelativistic reduction of the hadron matrix element for the scalar and the time part of the vector interaction shows that they both reduce simply to constants in leading order. However, under charge conjugation the matrix element $(\bar{\psi}_p C_S \psi_n)$ changes sign relative to $(\bar{\psi}_p C_V \gamma_4 \psi_n)$. Thus we write $\pm C_S$ in the ensuing formulae with the upper sign being for electron emission and the lower sign for positron emission. The lepton matrix elements are different in the two terms in Eq. (23) so the contribution to the shape-correction function from the scalar interaction will involve a different combination of electron and neutrino radial functions than that from the vector interaction. The final formula for $C(Z, W)$ is

$$C(Z, W) = \sum_{k_e k_\nu K} \lambda_{k_e} \left\{ (M_K(k_e, k_\nu) + \bar{m}_K(k_e, k_\nu))^2 \right.$$

$$\begin{aligned}
& + (m_K(k_e, k_\nu) + \overline{M}_K(k_e, k_\nu))^2 \\
& - \frac{2\mu_{k_e}\gamma_{k_e}}{k_e W} (M_K(k_e, k_\nu) + \overline{m}_K(k_e, k_\nu)) \\
& (m_K(k_e, k_\nu) + \overline{M}_K(k_e, k_\nu)) \}, \tag{24}
\end{aligned}$$

where $M_K(k_e, k_\nu)$ and $m_K(k_e, k_\nu)$ are the reduced matrix elements given in Eq. (A13), which incorporate the radial functions, $F(r)$ and $f(r)$, defined in Eq. (A14). The reduced matrix elements $\overline{M}_K(k_e, k_\nu)$ and $\overline{m}_K(k_e, k_\nu)$ are the same as $M_K(k_e, k_\nu)$ and $m_K(k_e, k_\nu)$ except that the radial functions, $F(r)$ and $f(r)$, are replaced by $\overline{F}(r)$ and $\overline{f}(r)$, where

$$\begin{aligned}
\overline{F}(r) &= H(r) \{-G_{--} j_{k_\nu-1}(p_\nu r) + G_{-+} j_{k_\nu}(p_\nu r)\} \\
&+ D(r) \{G_{+-} j_{k_\nu-1}(p_\nu r) - G_{++} j_{k_\nu}(p_\nu r)\} \\
\overline{f}(r) &= h(r) \{-G_{--} j_{k_\nu-1}(p_\nu r) + G_{-+} j_{k_\nu}(p_\nu r)\} \\
&+ d(r) \{G_{+-} j_{k_\nu-1}(p_\nu r) - G_{++} j_{k_\nu}(p_\nu r)\}. \tag{25}
\end{aligned}$$

The functions H , D , h and d are linear combinations of the electron functions, $f_\kappa(r)$ and $g_\kappa(r)$, as given in Eq. (A15); and the angular momentum factors $G_{\pm\pm}$ are defined in Eq. (A16).

1. Order of magnitude estimates

For a pure Fermi transition, the multipolarity of the transition operators is $K = 0$. Keeping only the lowest lepton partial waves, $k_e = 1$ and $k_\nu = 1$, we expand the lepton radial functions in a power series in r . The order of magnitude of the lepton wave functions at small r are

$$\begin{aligned}
f_1(r) &= 1 - \dots \\
g_{-1}(r) &= 1 - \dots \\
f_{-1}(r) &= \textit{small} \\
g_1(r) &= \textit{small} \\
j_0(p_\nu r) &= 1 - \dots \\
j_1(p_\nu r) &= \textit{small}, \tag{26}
\end{aligned}$$

We retain only $f_1(r)$, $g_{-1}(r)$ and $j_0(p_\nu r)$, setting their values to unity, and drop the other small terms. The angular momentum factors for $K = L = s = 0$ are $G_{++} = G_{--} = 1$, and

$G_{+-} = G_{-+} = 0$. Then the amplitudes become

$$\begin{aligned}
M_0(1, 1) &= C_V M_F + \dots \\
m_0(1, 1) &= \text{small}, \\
\overline{M}_0(1, 1) &= \mp C_S M_F + \dots \\
\overline{m}_0(1, 1) &= \text{small},
\end{aligned}
\tag{27}$$

where M_F is the Fermi matrix element. The shape-correction function is then

$$\begin{aligned}
C(Z, W) &= |M_F|^2 \left(C_V^2 + C_S^2 \pm \frac{2\mu_1\gamma_1}{W} C_S C_V \right) \\
&\simeq |M_F|^2 C_V^2 (1 + b_F \gamma_1 / W + \dots),
\end{aligned}
\tag{28}$$

where it is assumed that $C_S \ll C_V$. The term in $b_F \gamma_1 / W$ is called the Fierz interference term, with $b_F = \pm 2\mu_1 C_S / C_V$. This is the well-known expression given by Jackson, Treiman and Wyld [165]. Here μ_1 is one of the beta-decay Coulomb functions, Eq. (A9), and is of order unity, and $\gamma_1 = (1 - (\alpha Z)^2)^{1/2}$.

2. Determining a limit on C_S/C_V

With the results of our data survey, we can now search for any evidence of a $1/W$ term in the shape-correction function, and hence set a limit on C_S . The test is based on the corrected $\mathcal{F}t$ values being a constant for all superallowed transitions between isospin $T = 1$ analogue states. For optimum sensitivity, we do not use Eq. (28) for $C(Z, W)$ in the evaluation of the statistical rate function, f , because of the extreme nature of some of the approximations made in deriving that equation. Instead we use the exact numerically computed expression. Since this calculated value of f depends on the value of C_S we simply treat C_S as an adjustable parameter and seek a value that minimizes χ^2 , in a least-squares fit to the expression $\mathcal{F}t = \text{constant}$. The result is

$$C_S/C_V = -(0.00005 \pm 0.00130).
\tag{29}$$

The sign of C_S/C_V is determined from the fit, since the calculated f depends on the interference between vector and scalar interactions. The interpretation of the sign is a little more delicate. We define C_S to be the strength of the scalar interaction in electron-emission beta decay, and this is the value quoted in Eq. (29). Since all the superallowed data involve

positron emitters there is a sign change mentioned earlier due to charge conjugation that operationally is included in the computations. The corresponding Fierz interference constant, b_F , is just -2 times this quantity³: $b_F = 0.0001 \pm 0.0026$. Had we not assumed that parity was violated maximally then the outcome would be

$$\frac{C_S C_V + C'_S C'_V}{|C_V|^2 + |C'_V|^2 + |C_S|^2 + |C'_S|^2} = -(0.00005 \pm 0.00130). \quad (30)$$

This result shows a factor of 30 reduction in the central value compared to our previously published result [1], with the standard deviation being essentially unchanged. This is by far the most stringent limit on C_S/C_V ever obtained from nuclear beta decay.

D. Induced Scalar Interaction

If we consider only the vector part of the weak interaction, for composite spin-1/2 nucleons the most general form of that interaction is written [166] as

$$H_V = \bar{\psi}_p (g_V \gamma_\mu - f_M \sigma_{\mu\nu} q_\nu + i f_S q_\mu) \psi_n \bar{\phi}_e \gamma_\mu (1 + \gamma_5) \phi_{\bar{\nu}_e}, \quad (31)$$

with q_μ being the four-momentum transfer, $q_\mu = (p_p - p_n)_\mu$. The values of the coupling constants g_V (vector), f_M (weak magnetic) and f_S (induced scalar) are prescribed if the CVC hypothesis – that the weak vector current is just an isospin rotation of the electromagnetic vector current – is correct. In particular, since CVC implies that the vector current is divergenceless, we anticipate that $f_S = 0$. An independent argument [167], that there be no second-class currents in the hadronic weak interaction, also requires f_S to vanish. Our goal in this section is to use the data from superallowed beta decay to set limits on the possible value of the induced scalar coupling constant, f_S . This will provide a test of the CVC hypothesis and simultaneously set limits on the presence of second-class currents in the hadronic vector weak interaction.

³ In our previous work described in ref. [4] and adopted in our subsequent publications, we explicitly included a minus sign in the formulae in recognition that all the superallowed Fermi transitions involved positron emitters. Thus the shape-correction function $C(Z, W)$ was modified to $C(Z, W)(1 - \gamma_1 b_F/W)$ and a fit of $\mathcal{F}t(1 - \gamma_1 b_F/W)$ to a constant yielded a value of b_F that was negative. Currently in Eq. (28) we have defined b_F such that $C(Z, W)$ is modified to $C(Z, W)(1 + \gamma_1 b_F/W)$ and hence we are now quoting b_F with a positive sign.

1. *Relation between f_S and C_S*

Considering, then, just the induced scalar term in the vector part of the weak interaction,

$$H_V(S) = \bar{\psi}_p(i f_S q_\mu) \psi_n \bar{\phi}_e \gamma_\mu (1 + \gamma_5) \phi_{\bar{\nu}_e}, \quad (32)$$

we see that this term can be reorganised to match closely the Hamiltonian from the fundamental scalar interaction shown in Eq. (22). The momentum transfer, $q_\mu = (p_p - p_n)_\mu = -(p_e + p_{\bar{\nu}_e})_\mu$, can be moved into the lepton matrix element where, in combination with γ_μ , it can be replaced with the free-particle Dirac equation: $\gamma_\mu(p_e)_\mu \phi_e = i m_e \phi_e$, $\gamma_\mu(p_{\bar{\nu}_e})_\mu \phi_{\bar{\nu}_e} = i m_{\bar{\nu}_e} \phi_{\bar{\nu}_e}$, with m_e and $m_{\bar{\nu}_e}$ being the electron and neutrino masses, respectively. On setting the neutrino mass to zero, we find that $H_V(S)$ becomes

$$H_V(S) = \bar{\psi}_p m_e f_S \psi_n \bar{\phi}_e (1 + \gamma_5) \phi_{\bar{\nu}_e}. \quad (33)$$

This expression is equivalent to the fundamental scalar interaction in Eq. (22) with C_S simply replaced by $m_e f_S$. Thus, its effect on the shape-correction function can be described by the same replacement in Eq. (28). An equivalent result was obtained by Holstein [168].

2. *Determining a limit on f_S*

We have now established the mathematical equivalence of the effects that f_S and C_S have on the shape-correction function, $C(Z, W)$. As a result, we can use Eq. (29) to conclude that

$$m_e f_S / g_V = -(0.00005 \pm 0.00130). \quad (34)$$

The sign of f_S / g_V follows the same convention as that described after Eq. (29). This result is a vindication for the CVC hypothesis, which predicts $g_V = 1$ and $f_S = 0$. Our result confirms this prediction at the level of 13 parts in 10^4 . As already mentioned, this result can also be interpreted as setting a limit on vector second-class currents in the semi-leptonic weak interaction, which therefore have not been observed here at the same level of precision.

E. Right-hand Currents

Let us no longer consider parity violation to be maximal. The general form of the weak interaction Hamiltonian [165] for just the vector couplings of relevance for superallowed beta

decay is

$$H_V = (\bar{\psi}_p \gamma_\mu \psi_n)(C_V \bar{\phi}_e \gamma_\mu \phi_{\bar{\nu}_e} + C'_V \bar{\phi}_e \gamma_\mu \gamma_5 \phi_{\bar{\nu}_e}) \quad (35)$$

With $C'_V \neq C_V$ we cannot associate the coupling constants with the hadron matrix elements as we did in Eq. (23). Instead, the lepton and neutrino radial functions remain combined with C_V or C'_V . The final formula for the shape-correction function then becomes

$$C(Z, W) = \sum_{k_e k_\nu K} \lambda_{k_e} \left\{ \frac{1}{2} \left(M_K^2(k_e, k_\nu) + m_K^2(k_e, k_\nu) + N_K^2(k_e, k_\nu) + n_K^2(k_e, k_\nu) \right) - \frac{2\mu_{k_e} \gamma_{k_e}}{k_e W} \frac{1}{2} \left(M_K(k_e, k_\nu) m_K(k_e, k_\nu) + N_K(k_e, k_\nu) n_K(k_e, k_\nu) \right) \right\} \quad (36)$$

where $M_K(k_e, k_\nu)$, $m_K(k_e, k_\nu)$, $N_K(k_e, k_\nu)$, and $n_K(k_e, k_\nu)$ are reduced matrix elements as defined in Eq. (A13), with their respective radial functions being $F(r)$, $f(r)$, $G(r)$, and $g(r)$. These radial functions are

$$\begin{aligned} F(r) &= H(r) \{C_V G_{--} j_{k_\nu-1}(p_\nu r) - C'_V G_{-+} j_{k_\nu}(p_\nu r)\} \\ &\quad + D(r) \{C'_V G_{-+} j_{k_\nu-1}(p_\nu r) - C_V G_{++} j_{k_\nu}(p_\nu r)\} \\ f(r) &= h(r) \{C_V G_{--} j_{k_\nu-1}(p_\nu r) - C'_V G_{-+} j_{k_\nu}(p_\nu r)\} \\ &\quad + d(r) \{C'_V G_{-+} j_{k_\nu-1}(p_\nu r) - C_V G_{++} j_{k_\nu}(p_\nu r)\} \\ G(r) &= H(r) \{-C'_V G_{--} j_{k_\nu-1}(p_\nu r) + C_V G_{-+} j_{k_\nu}(p_\nu r)\} \\ &\quad + D(r) \{-C_V G_{-+} j_{k_\nu-1}(p_\nu r) + C'_V G_{++} j_{k_\nu}(p_\nu r)\} \\ g(r) &= h(r) \{-C'_V G_{--} j_{k_\nu-1}(p_\nu r) + C_V G_{-+} j_{k_\nu}(p_\nu r)\} \\ &\quad + d(r) \{-C_V G_{-+} j_{k_\nu-1}(p_\nu r) + C'_V G_{++} j_{k_\nu}(p_\nu r)\} \end{aligned} \quad (37)$$

where the functions H , D , h and d are linear combinations of the electron functions, $f_\kappa(r)$ and $g_\kappa(r)$ as given in Eq. (A15). The angular momentum factors $G_{\pm, \pm}$ are defined in Eq. (A16).

1. Order of magnitude estimates

Consider a pure Fermi transition for which the multipolarity is $K = 0$ and only the lowest lepton partial waves, $k_e = 1$ and $k_\nu = 1$, are kept. Then, as in Sect. IV C 1, the amplitudes become

$$M_0(1, 1) = C_V M_F + \dots$$

$$\begin{aligned}
m_0(1, 1) &= \text{small} \\
N_0(1, 1) &= -C'_V M_F + \dots \\
n_0(1, 1) &= \text{small},
\end{aligned} \tag{38}$$

The shape-correction function is then

$$C(Z, W) = |M_F|^2 \frac{1}{2} (C_V^2 + C'_V{}^2). \tag{39}$$

We see that the dominant impact of the right-hand current is simply to scale the statistical rate function by $\frac{1}{2}(1 + C_V'^2/C_V^2)$. This has no impact on the CVC test that demonstrates that $\mathcal{F}t = \text{constant}$, but it does shift the value of the vector coupling constant and thus the deduced value of V_{ud}^2 . However, V_{ud}^2 is obtained from the ratio of beta-decay to muon-decay rates, so before we can make any definitive statement on the effect of a right-hand current on V_{ud}^2 , we must first examine the impact of that current on muon decay. We will show next that the correction due to a right-hand current is second order in small quantities in muon decay, but first order in vector beta decay. To this end we examine a more general Hamiltonian presented by Herczeg [169].

2. The effect on V_{ud}^2

In the $SU(2)_L \times U(1)$ Standard Model, the semi-leptonic weak interaction Hamiltonian can be written schematically as

$$H_{SM} = \frac{G_F}{\sqrt{2}} V_{ud} (V - A)(V - A), \tag{40}$$

where the first factor of $V - A$ represents the lepton currents: $V = \bar{\phi}_e \gamma_\mu \phi_{\bar{\nu}_e}$ and $-A = \bar{\phi}_e \gamma_\mu \gamma_5 \phi_{\bar{\nu}_e}$, while the second $V - A$ represents the hadron currents: $V = \bar{\psi}_p \gamma_\mu \psi_n$ and $-A = \bar{\psi}_p \gamma_\mu \gamma_5 \psi_n$. The weak interaction coupling $G_F/\sqrt{2} = g^2/8M_W^2$, where g is the basic coupling constant of the Weinberg-Salam Standard Model and M_W is the mass of the exchanged W -boson.

Herczeg [169, 170] considers an extension that is the most general form for non-derivative local four-fermion couplings

$$\begin{aligned}
H &= a_{LL}(V - A)(V - A) + a_{LR}(V - A)(V + A) \\
&\quad + a_{RL}(V + A)(V - A) + a_{RR}(V + A)(V + A),
\end{aligned} \tag{41}$$

where again the first factor represents the lepton currents, the second the hadron currents. The lepton fields are now written as $V = \bar{\phi}_e \gamma_\mu \phi_{\nu_e}^L$ or $\bar{\phi}_e \gamma_\mu \phi_{\nu_e}^R$ depending whether the chirality of the neutrino is left-handed for $V - A$ coupling or right-handed for $V + A$ coupling. The neutrino states are in general linear combinations of mass eigenstates,

$$\phi_{\nu_e}^L = \sum_i U_{ei} \phi_i^L \quad \phi_{\nu_e}^R = \sum_i V_{ei} \phi_i^R, \quad (42)$$

where U_{ei} and V_{ei} are first-row elements of the neutrino mixing matrix. The observed beta decay probability is the sum of the probabilities of decays into the energetically allowed neutrino mass eigenstates. We follow Herczeg [169, 170] in assuming that the neutrinos produced in beta decay are light enough that the effects of their masses can be neglected. In particular, the terms that arise from the interference between amplitudes involving neutrinos of different chirality are dropped. Then the effect of neutrino mass mixing can be taken into account by our multiplying the coupling constants a_{LL} and a_{LR} by $\sqrt{u_e}$, and a_{RL} and a_{RR} by $\sqrt{v_e}$ where

$$u_e = \sum'_i |U_{ei}|^2 \quad v_e = \sum'_i |V_{ei}|^2. \quad (43)$$

The prime on the summation indicates that the sum extends only over the neutrinos that are light enough to be produced in beta decay. Note that if all the neutrinos are light for both left-handed and right-handed chiralities, then $u_e = v_e = 1$ as a consequence of the unitarity of the neutrino mixing matrix.

Herczeg's Hamiltonian, Eq. (41), can be rewritten

$$\begin{aligned} H &= (a_{LL} + a_{LR} + a_{RL} + a_{RR})VV \\ &\quad + (-a_{LL} - a_{LR} + a_{RL} + a_{RR})AV \\ &\quad + (-a_{LL} + a_{LR} - a_{RL} + a_{RR})VA \\ &\quad + (a_{LL} - a_{LR} - a_{RL} + a_{RR})AA \end{aligned} \quad (44)$$

We can compare this with the Jackson, Treiman and Wyld (JTW) Hamiltonian [165], which in the current notation becomes

$$\begin{aligned} H_{JTW} &= (C_V V - C'_V A)V + (-C_A A + C'_A V)A \\ &= C_V VV - C'_V AV + C'_A VA - C_A AA \end{aligned} \quad (45)$$

Thus we identify the correspondences as⁴

$$\begin{aligned}
C_V &= a_{LL} + a_{LR} + a_{RL} + a_{RR} \\
C'_V &= a_{LL} + a_{LR} - a_{RL} - a_{RR} \\
C_A &= -a_{LL} + a_{LR} + a_{RL} - a_{RR} \\
C'_A &= -a_{LL} + a_{LR} - a_{RL} + a_{RR}
\end{aligned} \tag{46}$$

For Fermi beta decay, only the vector part of the weak hadron current contributes, so the decay rate, Γ_β , as shown earlier in Eq. (39), is proportional to

$$\begin{aligned}
\Gamma_\beta &\propto \frac{1}{2} (|C_V|^2 + |C'_V|^2) \\
&= |a_{LL} + a_{LR}|^2 + |a_{RL} + a_{RR}|^2 \\
&= |a_{LL}|^2 (|1 + \bar{a}_{LR}|^2 + |\bar{a}_{RL} + \bar{a}_{RR}|^2) \\
&\simeq |a_{LL}|^2 (1 + 2Re\bar{a}_{LR} + \dots)
\end{aligned} \tag{47}$$

where $\bar{a}_{ij} = a_{ij}/a_{LL}$.

To continue our determination of V_{ud} we need to consider the purely leptonic muon decay. Herczeg [169] writes the effective Hamiltonian for muon decay in analogy to Eq. (41) as

$$\begin{aligned}
H &= c_{LL}(V - A)(V - A) + c_{LR}(V - A)(V + A) \\
&\quad + c_{RL}(V + A)(V - A) + c_{RR}(V + A)(V + A)
\end{aligned} \tag{48}$$

The coupling constants in Eqs. (48) and (41) are related by the CKM matrix elements by

$$\begin{aligned}
a_{LL} &= c_{LL}V_{ud}^L \\
a_{LR} &= c_{LR}e^{i\alpha}V_{ud}^R \\
a_{RL} &= c_{RL}V_{ud}^L \\
a_{RR} &= c_{RR}e^{i\alpha}V_{ud}^R.
\end{aligned} \tag{49}$$

Here V_{ud}^L is the ud -matrix element of the CKM matrix for left-handed chirality quarks, and V_{ud}^R is for right-handed chirality quarks. The phase α is a CP-violating phase in the

⁴ Herczeg [169, 170] employs a metric that leads to a different sign on the γ_5 matrix, so his correspondences yield a different overall sign from ours for C'_V and C_A .

right-handed CKM matrix. The decay rate, Γ_μ , for muon decay is proportional to

$$\begin{aligned}\Gamma_\mu &\propto |c_{LL}|^2 + |c_{LR}|^2 + |c_{RL}|^2 + |c_{RR}|^2 \\ &= |c_{LL}|^2 \left(1 + |\bar{c}_{LR}|^2 + |\bar{c}_{RL}|^2 + |\bar{c}_{RR}|^2\right)\end{aligned}\quad (50)$$

where $\bar{c}_{ij} = c_{ij}/c_{LL}$.

Combining Eqs. (47) and (50), we obtain an expression that connects the ratio of beta-decay to muon-decay rates with the value of $|V_{ud}^L|^2$, *viz.*

$$\frac{\Gamma_\beta}{\Gamma_\mu} = |V_{ud}^L|^2 \frac{|1 + \bar{a}_{LR}|^2 + |\bar{a}_{RL} + \bar{a}_{RR}|^2}{1 + |\bar{c}_{LR}|^2 + |\bar{c}_{RL}|^2 + |\bar{c}_{RR}|^2}.\quad (51)$$

In the Standard Model, only a_{LL} and c_{LL} are non-zero; in any case, the quantities \bar{a}_{ij} and \bar{c}_{ij} with $ij = LR, RL, \text{ or } RR$ can certainly be considered small. The correction to the muon decay rate from right-handed interactions is therefore seen to be second order in small quantities, while the correction to Fermi beta decay rate is first order. Keeping only first-order small quantities, Eq. (51) reduces to⁵

$$\frac{\Gamma_\beta}{\Gamma_\mu} = |V_{ud}^L|^2 (1 + 2Re\bar{a}_{LR}).\quad (52)$$

If the neutrino masses are such that $u_e \neq 1$ and $v_e \neq 1$ then this equation is modified to

$$\frac{\Gamma_\beta}{\Gamma_\mu} = |V_{ud}^L|^2 \frac{(u_e)_\beta}{[(u_e)_\mu (u_\mu)_\mu]^{1/2}} (1 + 2Re\bar{a}_{LR}),\quad (53)$$

where $(u_e)_\beta$ in the numerator is given by the u_e in Eq. (43), with the sum extended over neutrinos light enough to be produced in beta decay, while in the denominator $(u_e)_\mu$ is given by the same expression but with the sum extended over neutrinos light enough to be produced in muon decay. Note that the Q -value for muon decay is 105 MeV, a factor of ten times larger than the Q -value for any Fermi beta decay we are considering. Also u_μ in Eq. (53) is defined as $\sum_i' |U_{\mu i}|^2$, where $U_{\mu i}$ are second-row elements of the neutrino mixing matrix. In what follows, we will assume $(u_e)_\beta = (u_e)_\mu = (u_\mu)_\mu = 1$.

Before proceeding to numeric limits, it is worth showing how the current formulae relate to the simpler and more restrictive manifest left-right symmetric model [171]. In this model

⁵ Herczeg [170] also considers the possibility that the relation between purely leptonic and semi-leptonic Hamiltonians, Eq. (49), is not sufficiently general. He writes $a_{LL} = (a_{LL})_{SM} + a'_{LL}$, with $(a_{LL})_{SM} = c_{LL}V_{ud}^L$. Then Eq. (52) becomes $\Gamma_\beta/\Gamma_\mu = |V_{ud}^L|^2(1 + 2Re(\bar{a}'_{LL} + \bar{a}_{LR}))$, where $\bar{a}'_{LL} = a'_{LL}/(a_{LL})_{SM}$. We will not pursue this further, but it is obvious the formulae above can accommodate this extension with a simple replacement of \bar{a}_{LR} with $\bar{a}'_{LL} + \bar{a}_{LR}$.

the departure from maximal parity violation is entirely due to the presence of a second W -boson whose mass is much heavier than the usual W -boson. If left-hand couplings are mediated by the boson, W_L , and right-hand couplings by W_R , then W_L and W_R will be linear combinations of the mass eigenstates W_1 and W_2 , *viz.*

$$\begin{aligned} W_L &= W_1 \cos \zeta + W_2 \sin \zeta \\ W_R &= e^{i\omega} (-W_1 \sin \zeta + W_2 \cos \zeta) \end{aligned} \quad (54)$$

and ω is a CP violating phase. If it is further assumed that, apart from the different masses of the W_1 and W_2 bosons, the coupling constants and CKM matrix elements are identical for left-hand and right-hand couplings, then there are only two parameters in this model. These parameters are: $\delta = (m_1/m_2)^2$ and ζ , where m_1 and m_2 are the masses of W_1 and W_2 respectively. Both parameters are small and, of course, are zero in the Standard Model. The parameters of Herczeg's Hamiltonian, Eq. (41), can be expressed in terms of δ and ζ [170]:

$$\begin{aligned} a_{LL} &= \frac{g^2}{8m_1^2} V_{ud}^L & \bar{a}_{RR} &= \delta \\ \bar{a}_{LR} &= \bar{a}_{RL} = -e^{i\omega} \zeta \rightarrow -\zeta \end{aligned} \quad (55)$$

for negligible CP-violating effects. In this limit, the expression for the ratio of Fermi beta to muon decay rates, Eq. (52), reduces to

$$\frac{\Gamma_\beta}{\Gamma_\mu} = |V_{ud}^L|^2 (1 - 2\zeta). \quad (56)$$

This is the expression we used in our earlier work [1] to set limits on the extent of right-hand currents.

3. Numeric Limit

Let us now insert the experimental values from our survey data for the beta-decay and muon-decay rates to determine an experimental value for $|V_{ud}|^2$, which we will write as $|V_{ud}|_{\text{expt}}^2$. This is the value we recorded earlier in Eq. (17). Then Eq. (52) can be written as

$$\begin{aligned} |V_{ud}|_{\text{expt}}^2 &= |V_{ud}^L|^2 (1 + 2Re\bar{a}_{LR}) \\ &= (1 - |V_{us}^L|^2 - |V_{ub}^L|^2) (1 + 2Re\bar{a}_{LR}), \end{aligned} \quad (57)$$

where in the second line we have inserted the condition for unitarity of the CKM matrix. Adopting the PDG's recommended values [7] for $|V_{us}^L|$ and $|V_{ub}^L|$ (see text preceding Eq. (19)) we obtain the following result from Eq. (57):

$$\begin{aligned} (0.9482 \pm 0.0008) &= (0.9516 \pm 0.0011)(1 + 2\text{Re}\bar{a}_{LR}) \\ \text{Re}\bar{a}_{LR} &= -0.00176 \pm 0.00074. \end{aligned} \tag{58}$$

Within the context of the manifest left-right symmetric model (see Eq. 56), this result corresponds to $\zeta = 0.00176 \pm 0.00074$, a similar value to the one we reported previously [1]. The result of a non-zero a_{LR} or ζ simply reflects the fact that the experimental values of the first-row CKM matrix elements do not satisfy the unitarity requirement.

If, instead, we adopt the E865 value [2] for V_{us} rather than the PDG average, then the result in Eq. (58) is modified to

$$\begin{aligned} (0.9482 \pm 0.0008) &= (0.9484 \pm 0.0014)(1 + 2\text{Re}\bar{a}_{LR}) \\ \text{Re}\bar{a}_{LR} &= -0.00007 \pm 0.00084. \end{aligned} \tag{59}$$

This result is consistent with no right-hand currents and unitarity being satisfied in the experimental CKM matrix elements.

V. CONCLUSIONS

Previous surveys of superallowed Fermi beta decay have at times noted disagreement [3, 5] among the derived $\mathcal{F}t$ values, and at other times agreement [4, 6]. When disagreement was evident, subsequent attention paid to the problem led to both theoretical and experimental advances. As presented here, in Sect. III, the status now is of excellent agreement among all $\mathcal{F}t$ values – to better than 3 parts in 10^4 over a wide range of nuclei from $A = 10$ to $A = 74$. Such agreement confirms the expectations of CVC, allows very restrictive limits to be set on the possible presence of scalar currents and makes it possible to go forward with confidence to the next steps – the determination of V_{ud} and the unitarity test of the CKM matrix.

The outstanding challenge at this time is that the value obtained for V_{ud} , when combined with the current PDG-recommended values of V_{us} and V_{ub} , leads to a unitarity test that fails by more than two standard deviations. There are no evident defects in the calculated

radiative and isospin-symmetry-breaking corrections that could remove this problem and, indeed, a shift in any one of these corrections large enough to restore unitarity would be almost impossible to justify [1]. Moreover, the derived value of V_{ud} from nuclear decays has been remarkably stable for three decades despite a vast increase in the quantity of high quality data and many theoretical refinements in the calculations of the correction terms.

So if any progress is to be made in firmly establishing (or eliminating) the discrepancy with unitarity, both theory and experiment must be brought to bear afresh on the principal sources of uncertainty. Although we will focus here on improving the nuclear contribution to the unitarity test, additional experiments are also required for neutron, pion and kaon decays. The first two provide independent, though so far much less precise, values for V_{ud} ; the third establishes the value of V_{us} , which may ultimately turn out to be solely responsible for restoring the CKM matrix to unitarity. Whatever the outcome for unitarity, however, the results of all these studies will provide crucial information, either in characterizing new physics beyond the standard model or in setting a tight limit on its possible existence.

We have taken pains throughout this work to pay careful attention to all uncertainties, theoretical and experimental. In Section IV A we detailed the various contributions to the uncertainty in $|V_{ud}|^2$. Of these, by far the largest is due to the nucleus-independent radiative correction, Δ_R^V . Its uncertainty arises primarily from a box diagram involving the exchange of one W boson and one photon between the hadron and the lepton. To make the loop integration tractable, it is divided by a scale parameter into high- and low-energy portions. The high-energy contribution can be computed reliably [172] but the low-energy one, as calculated originally by Sirlin [173], depends on the choice of scale parameter. Sirlin chose [163, 164] a reasonable range for this parameter, which has been retained by subsequent authors [174, 175]. It is this choice of range that drives the overall uncertainty on Δ_R^V . Recent work [176] with effective field theories based on chiral perturbation theory has been unable to improve the situation: although this approach replaces the low-energy contributions to the loop diagrams by well-defined low-energy constants, the values of these constants are not known *a priori*. How to obtain a more refined, first-principles computation of the low-energy contribution remains an open theoretical problem [172], but one of considerable importance and urgency. Not only is this uncertainty the principal limitation on the precision with which V_{ud} can be determined from nuclear superallowed β decay, but it will have a similar limiting effect on its determination from neutron and pion decays as well.

The next largest contributor to the error budget on $|V_{ud}|^2$ is the isospin-symmetry-breaking correction, δ_C . Although uncertainties have been individually determined for the most recent calculations [158] of $\delta_C - \delta_{NS}$ (see Table IX), the dominant source of $|V_{ud}|^2$ uncertainty attributable to δ_C arises from the small systematic difference between the results from different theoretical techniques used to calculate δ_C . Our approach [158], using Woods-Saxon functions, yields larger δ_C values than the Ormand-Brown one [159], using Hartree-Fock functions. Here we have taken the democratic approach, considering that these two sets of calculations are equally likely to be correct and letting the difference between their results determine a systematic uncertainty that we apply to the final result (see Eq. (12)).

If reducing the uncertainty on Δ_R^V must rank as the first priority for future theoretical work, then improving our confidence in δ_C can be taken as the top priority challenge for experiment. Although there is no way to check the correctness of the absolute values of δ_C from experiment, it is possible to check the nucleus-to-nucleus variations in the calculated values. The method, which is illustrated in Fig. 4, is based on the validity of the CVC hypothesis that the corrected $\mathcal{F}t$ values for the superallowed $0^+ \rightarrow 0^+$ decays should be constant. In the figure we compare the uncorrected measured ft values (points and error bars) with the theoretical quantity $\overline{\mathcal{F}t}/((1+\delta'_R)(1-\delta_C+\delta_{NS}))$ shown as a band, the width of which represents its estimated error. With the average $\mathcal{F}t$ value, $\overline{\mathcal{F}t}$, taken from Table IX, this comparison specifically tests the collective ability of all three calculated correction terms to reproduce the variations in ft from one transition to another. However, since δ'_R is almost independent of Z when $Z > 10$, this test really probes directly the effectiveness of the calculated values of $\delta_C - \delta_{NS}$.

It can be seen that there is remarkable agreement between theory and experiment. In assessing the significance of this agreement, it is important to recognize that the calculations of δ_C and δ_{NS} for $Z \leq 26$ are based on well-established shell-model wave functions and were further tuned to reproduce measured binding energies, charge radii and coefficients of the isobaric multiplet mass equation [158]. The origins of the calculated correction terms for all cases are completely independent of the superallowed decay data. Thus, the agreement in the figure between the measured superallowed data points and the theoretical band is already a powerful validation of the calculated corrections used in determining that band. The validation becomes even more convincing when we consider that it would require a

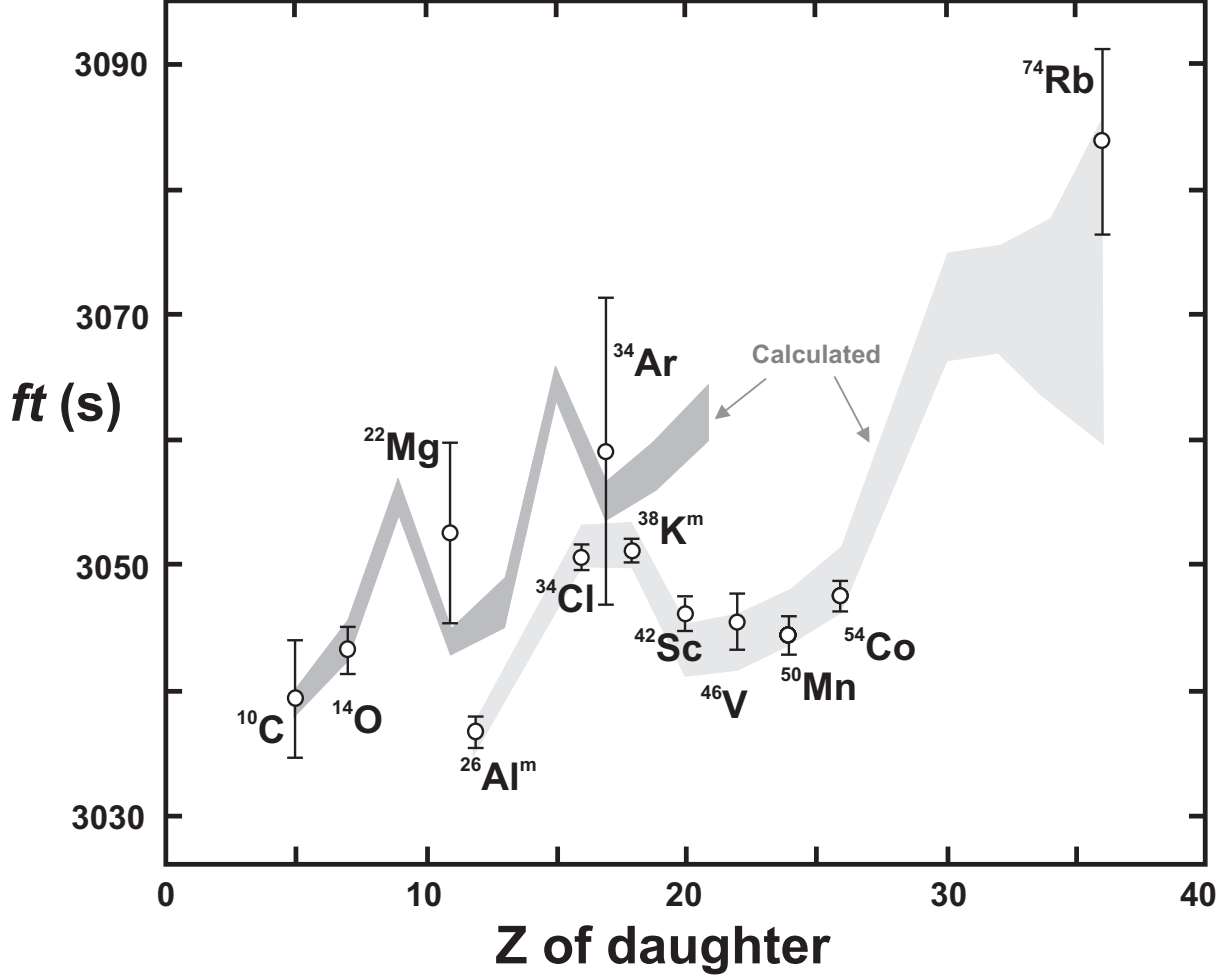


FIG. 4: Experimental ft values plotted as a function of the charge on the daughter nucleus, Z . The bands represent the theoretical quantity $\overline{ft}/((1 + \delta'_R)(1 - \delta_C + \delta_{NS}))$. The two groups distinguish those beta emitters whose parent nuclei have isospin $T_z = -1$ (darker shading) from those with $T_z = 0$ (lighter shading).

pathological fault indeed in the theory to allow the observed nucleus-to-nucleus variations in δ_C to be reproduced in such detail while failing to obtain the *absolute* values to comparable precision. Pleasing as the agreement in Fig. 4 is, though, new experiments can still improve the test, making it even more demanding, and can ultimately reduce the uncertainty in δ_C further.

These new experiments can follow different paths. One is to improve the precision on the nine superallowed transitions whose ft values are already known to within 0.15% or better. On the one hand, these are the easiest cases to study, all having stable daughters and all,

except ^{10}C , decaying predominantly ($> 99\%$) through a single superallowed transition. On the other hand, they have been the subject of intense scrutiny for at least the past four decades and, given the number of careful measurements already published, the prospects for really significant improvements in these cases, at least in the near future, do not seem bright. Nevertheless, a glance at Fig. 2 shows that some modest improvements are certainly possible. If we accept as a goal that experiment should be a factor of two more precise than theory, then we see that the Q_{EC} -values for ^{10}C , ^{14}O , $^{26}\text{Al}^m$, ^{42}Sc and ^{46}V , the half-lives of ^{10}C , $^{26}\text{Al}^m$, ^{42}Sc and ^{50}Mn , and the branching ratio for ^{10}C can all bear improvement.

A second path is to expand the number of precisely measured superallowed emitters to include cases for which the calculated nuclear-structure-dependent corrections are larger, or show larger variations from nuclide to nuclide, than the values applied to the nine currently best-known transitions. We argue that if the calculations reproduce the experimentally observed variations where they are large, then that must surely verify their reliability for the original nine transitions whose corrections are considerably smaller. The recent results for ^{22}Mg , ^{34}Ar and ^{74}Rb are the first cases of this type to reach sufficient precision that they can contribute to the test (see Fig. 4) but more are sure to follow. We have included in our survey all cases that we believe are potential candidates within the next few years.

Without doubt, these new cases present serious experimental challenges. In general, the parent nuclei are more exotic and thus more difficult to produce in pure and statistically useful quantities. They also exhibit more complex branching patterns, which for the cases with $A \geq 62$ include Gamow-Teller transitions that may be unobservable individually but collectively can play a non-negligible role [81]. These heavier nuclei also have very short half-lives, which currently limit the precision with which their Q_{EC} -values can be measured. Even so, all these obstacles are obviously now being overcome and we may reasonably hope that before long there will not only be more cases with precisely measured parameters, but there will be more than one measurement of each parameter, an essential prerequisite for reliable results at the level of precision needed to constrain the correction terms.

Although it would not impact significantly on the unitarity question, there is an additional reason to improve the precision with which the ft values are known, particularly for the cases with $A \leq 26$. A scalar current, if it exists, would manifest itself as a $1/W$ -dependence in the shape-correction function used in the f -value calculations (see Eq. (28)). Since the superallowed transition energies decrease with A , this effect would be strongest for the

lightest nuclei, ^{10}C and ^{14}O . Improved precision in the $\mathcal{F}t$ values for those two nuclei would act directly to reduce the limits set on a possible scalar current.

In conclusion, we can assert that world data for superallowed $0^+ \rightarrow 0^+$ β decays strongly support the CVC expectation of an unrenormalized vector coupling constant, and also set a new limit on the possible existence of scalar currents. The nuclear-structure-dependent corrections used in the analyses of these data have so far stood up very favorably to experimental tests, and the value currently obtained with them for V_{ud} is deemed to be very robust, even though it is an important component of the top-row test of CKM unitarity that fails by more than two standard deviations. We have indicated the improvements required from both theory and experiment to increase the precision in future so as to produce a more definitive result for the unitarity test.

Acknowledgments

The work of JCH was supported by the U. S. Dept. of Energy under Grant DE-FG03-93ER40773 and by the Robert A. Welch Foundation. IST would like to thank the Cyclotron Institute of Texas A & M University for its hospitality during several two-month visits.

APPENDIX A: STATISTICAL RATE FUNCTION

The statistical rate function is an integral over phase space,

$$f = \int_1^{W_0} pW(W_0 - W)^2 F(Z, W) S(Z, W) dW, \quad (\text{A1})$$

where W is the electron total energy in electron rest-mass units, W_0 is the maximum value of W , $p = (W^2 - 1)^{1/2}$ is the electron momentum, Z is the charge number of the daughter nucleus (positive for electron emission, negative for positron emission), $F(Z, W)$ is the Fermi function, and $S(Z, W)$ is the shape-correction function. If the shape-correction function is put to unity, the integral becomes the customarily defined one for beta decay, which we will denote as f_{stat} :

$$f_{\text{stat}} = \int_1^{W_0} pW(W_0 - W)^2 F(Z, W) dW. \quad (\text{A2})$$

The exact evaluation of f differs from f_{stat} by 0.2% at $A = 10$ up to 5.7% at $A = 74$. Thus, to maintain 0.1% accuracy for f over that range, we must determine the shape-correction

function itself with 2% accuracy. Obtaining this accuracy requires consideration of the following issues:

- The electron wave functions can no longer be simply those of the lowest partial wave ($j = 1/2$) generated by a point nuclear charge and evaluated at radius R , the nuclear surface, but must be the exact functions for some chosen nuclear charge-density distribution;
- The lepton wavefunctions exhibit some r^2 dependence over the nuclear volume, leading to what are called second-forbidden corrections. Furthermore, a more accurate treatment of the weak interaction leads to relativistic and induced-current corrections. All these effects must be incorporated since they impact on the nuclear matrix elements and inject a mild nuclear-structure dependence into the evaluation of f .
- The atomic electrons cannot be ignored, but must be accommodated approximately in a screening correction;

In what follows we describe the ingredients of a code we have written that incorporates these effects. It is based on the formalism of Behrens and Bühring [166]. Note that they define

$$F(Z, W)S(Z, W) = F_0L_0C(Z, W), \quad (\text{A3})$$

where $F_0 = 2F(Z, W)/(1 + \gamma_1)$. The purpose of their redefining the shape correction factor in this way was to remove the historic requirement to evaluate the electron wave functions at the nuclear surface. The product F_0L_0 is given entirely in terms of the amplitudes of the electron wave function at the origin (see Eq. (A9) below), and $C(Z, W)$ is the shape-correction function defined with respect to this choice.

1. Electron Radial Wave Functions

The wave function for the electron emitted in beta decay is given by the solution to the Dirac equation with an external electromagnetic field present, but restricted to the special case where the vector potential vanishes identically and the scalar potential is static and spherically symmetric. We solve in spherical coordinates and introduce a partial wave

expansion such that the basis states are written:

$$\psi_\kappa^\mu = \begin{pmatrix} \text{sign}(\kappa) f_\kappa(r) \chi_{-\kappa}^\mu \\ g_\kappa(r) \chi_\kappa^\mu \end{pmatrix}, \quad (\text{A4})$$

where f_κ , g_κ are radial functions, and χ_κ^μ are the usual spin-angular-momentum wave functions describing the coupling of the orbital angular momentum l and spin $\frac{1}{2}$ to give a total angular momentum j with z -component μ :

$$\chi_\kappa^\mu = i^l \sum_{m_l m_s} \langle l m_l \frac{1}{2} m_s | j \mu \rangle Y_{l m_l}(\hat{\mathbf{r}}) \chi_{m_s}. \quad (\text{A5})$$

The eigenvalue κ is

$$\kappa = -j(j+1) + l(l+1) - \frac{1}{4} \quad (\text{A6})$$

and has values

$$\begin{aligned} \kappa &= -(l+1) = -(j + \frac{1}{2}) & \text{if } j = l + \frac{1}{2} \\ \kappa &= l = (j + \frac{1}{2}) & \text{if } j = l - \frac{1}{2}. \end{aligned} \quad (\text{A7})$$

The radial functions are solutions to a pair of coupled equations

$$\begin{aligned} \frac{dg_\kappa}{dr} + \frac{(\kappa+1)}{r} g_\kappa - (W+1 - V(r)) f_\kappa &= 0 \\ \frac{df_\kappa}{dr} - \frac{(\kappa-1)}{r} f_\kappa + (W-1 - V(r)) g_\kappa &= 0. \end{aligned} \quad (\text{A8})$$

Here $V(r)$ is a spherically symmetric static potential that represents the interaction of the electron with the charge distribution of the nucleus.

Our task is to solve the pair of coupled radial equations, Eq. (A8), in three regions, $0 \leq r \leq R_1$, $R_1 \leq r \leq R_2$, $R_2 \leq r \leq \infty$, matching the solutions at each region boundary. The first region is the one over which the nuclear charge density is non-zero. Here, we establish a power-series solution, regular at the origin, as the starting solution and integrate numerically to R_1 . In the second region, we have a pure Coulomb potential, for which an analytic solution can be found in terms of confluent hypergeometric functions of complex argument. The asymptotic solution in the third region is expressed in terms of the desired outgoing waves and a phase shift. The unknowns in the calculation are the phase shift, Δ_κ , and the normalization of the interior solution, α_κ : they are determined from the matching conditions.

In the derivation of expressions for beta-decay observables, certain combinations of amplitudes and phase shifts characterising the electron wave functions appear. These combinations are called the beta-decay Coulomb functions, and are generally organized so that they are of order unity, with corrections of order $(\alpha Z)^2$. Since we are only interested here in the shape-correction function, the only such functions we need are $F_0 L_0$, λ_k and μ_k , where $k = |\kappa|$, which are defined as

$$\begin{aligned} F_0 L_0 &= \frac{\alpha_{-1}^2 + \alpha_{+1}^2}{2p^2} \\ \lambda_k &= \frac{\alpha_{-k}^2 + \alpha_{+k}^2}{\alpha_{-1}^2 + \alpha_{+1}^2} \\ \mu_k &= \frac{\alpha_{-k}^2 - \alpha_{+k}^2}{\alpha_{-k}^2 + \alpha_{+k}^2} \frac{kW}{\gamma_k}, \end{aligned} \tag{A9}$$

where $\gamma_k = \{k^2 - (\alpha Z)^2\}^{1/2}$. Although these functions have actually been tabulated by Behrens and Jänecke [177], we have not used the tables but, in the interests of precision, have explicitly computed the functions from the calculated values of α_κ .

2. Shape-correction function

Behrens and Bühring [166] give the following expression for the shape-correction function:

$$\begin{aligned} C(Z, W) &= \sum_{k_e k_\nu K} \lambda_{k_e} \left\{ M_K^2(k_e, k_\nu) + m_K^2(k_e, k_\nu) \right. \\ &\quad \left. - \frac{2\mu_{k_e} \gamma_{k_e}}{k_e W} M_K(k_e, k_\nu) m_K(k_e, k_\nu) \right\}, \end{aligned} \tag{A10}$$

where the sums over k_e and k_ν are partial-wave expansions of the electron and neutrino wave functions with $k_e = j_e + \frac{1}{2}$ and $k_\nu = j_\nu + \frac{1}{2}$, j_e and j_ν being the electron and neutrino total angular momenta. The integer K represents the multipolarity of the transition operators and is limited to the range $|j_e - j_\nu| \leq K \leq j_e + j_\nu$. The functions $M_K(k_e, k_\nu)$ and $m_K(k_e, k_\nu)$ are given in terms of form factors [166] and we evaluate these form factors in the ‘‘impulse approximation’’. In this approximation, the nucleus is treated as a collection of non-interacting nucleons so it is only necessary to consider the weak interaction as acting upon a single nucleon. All the many-body aspects of the nucleus can thus be handled in the standard shell-model way. Let O be a one-body operator, which can be written

$$O = \sum_{\alpha\beta} \langle \alpha | O | \beta \rangle a_\alpha^\dagger a_\beta, \tag{A11}$$

where a_α^\dagger is the creation operator for a nucleon in quantum state α , and a_β is an annihilation operator destroying a nucleon in state β . The matrix element of O for many-body states becomes

$$\langle f|O|i\rangle = \sum_{\alpha\beta} \langle \alpha|O|\beta\rangle \langle f|a_\alpha^\dagger a_\beta|i\rangle; \quad (\text{A12})$$

that is, the matrix element is a linear combination of single-particle matrix elements, $\langle \alpha|O|\beta\rangle$. The coefficients in the expansion, $\langle f|a_\alpha^\dagger a_\beta|i\rangle$, are called one-body density matrix elements (OBDME). We leave it, then, as the job of the shell model to provide the OBDMEs and only deal here with the single-particle matrix elements. The functions $M_K(k_e, k_\nu)$ and $m_K(k_e, k_\nu)$ are now given in terms of reduced nuclear matrix elements for a single-particle transition $j_\beta \rightarrow j_\alpha$ by

$$\begin{aligned} M_K(k_e, k_\nu) &= \frac{\sqrt{4\pi}}{\hat{K} \hat{J}_i} \sum_{Ls} (-)^{K-L} \langle j_\alpha \| F(r) \hat{T}_{KLs} \| j_\beta \rangle \\ m_K(k_e, k_\nu) &= \frac{\sqrt{4\pi}}{\hat{K} \hat{J}_i} \sum_{Ls} (-)^{K-L} \langle j_\alpha \| f(r) \hat{T}_{KLs} \| j_\beta \rangle, \end{aligned} \quad (\text{A13})$$

where \hat{j} is a short-hand notation for $(2j+1)^{1/2}$ and J_i is the spin of the decaying nucleus.

The radial functions are

$$\begin{aligned} F(r) &= H(r) \{G_{--} j_{k_\nu-1}(p_\nu r) - G_{-+} j_{k_\nu}(p_\nu r)\} \\ &\quad + D(r) \{G_{+-} j_{k_\nu-1}(p_\nu r) - G_{++} j_{k_\nu}(p_\nu r)\} \\ f(r) &= h(r) \{G_{--} j_{k_\nu-1}(p_\nu r) - G_{-+} j_{k_\nu}(p_\nu r)\} \\ &\quad + d(r) \{G_{+-} j_{k_\nu-1}(p_\nu r) - G_{++} j_{k_\nu}(p_\nu r)\}, \end{aligned} \quad (\text{A14})$$

with

$$\begin{aligned} H(r) &= \frac{1}{2} (f_{k_e}(r) + g_{-k_e}(r)) \\ D(r) &= \frac{1}{2} (g_{k_e}(r) - f_{-k_e}(r)) \\ h(r) &= \frac{1}{2} (f_{k_e}(r) - g_{-k_e}(r)) \\ d(r) &= \frac{1}{2} (g_{k_e}(r) + f_{-k_e}(r)). \end{aligned} \quad (\text{A15})$$

Here $f_\kappa(r)$ and $g_\kappa(r)$ are radial electron functions⁶, while the spherical Bessel functions represent radial neutrino wave functions. The functions G_{++} , G_{+-} , G_{-+} and G_{--} are

⁶ The internal normalisations at the origin are here set to unity. Recall that these normalisations, α_{κ} , have been separated out into the beta-decay Coulomb functions, $F_0 L_0$, (see Eq. (A9)).

short-hand notations for $G_{KLs}(k_e, k_\nu)$, $G_{KLs}(k_e, -k_\nu)$, $G_{KLs}(-k_e, k_\nu)$, and $G_{KLs}(-k_e, -k_\nu)$ respectively, where the functions $G_{KLs}(\kappa_e, \kappa_\nu)$ contain all the angular momentum factors for the leptons:

$$G_{KLs}(\kappa_e, \kappa_\nu) = i^{l_\nu + L + l_e} (-)^{j_e - j_\nu} \hat{s} \hat{K} \hat{j}_e \hat{j}_\nu \hat{l}_e \hat{l}_\nu \langle l_e 0 l_\nu 0 | L 0 \rangle \begin{Bmatrix} K & s & L \\ j_e & \frac{1}{2} & l_e \\ j_\nu & \frac{1}{2} & l_\nu \end{Bmatrix}. \quad (\text{A16})$$

Lastly, the operators \hat{T}_{KLs} depend on the angle and spin coordinates and are defined as

$$\begin{aligned} \hat{T}_{KLs}^M(\hat{\mathbf{r}}) &= (V_0 + A_0) i^L Y_{LM}(\hat{\mathbf{r}}) \delta_{K,L} & \text{if } s = 0 \\ &= (\mathbf{V} + \mathbf{A}) \cdot i^L \mathbf{Y}_{KLM}(\hat{\mathbf{r}}) & \text{if } s = 1, \end{aligned} \quad (\text{A17})$$

where V_0 , A_0 are the time parts of the vector and axial-vector hadronic currents and \mathbf{V} , \mathbf{A} are the space parts. Further $\mathbf{Y}_{KLM}(\hat{\mathbf{r}})$ is a vector spherical harmonic [178], which in Eq. (A17) forms a scalar product with vectors \mathbf{V} and \mathbf{A} .

3. Hadronic matrix element

For nucleons, the vector and axial-vector interactions are written

$$\begin{aligned} V_\mu &= g_V \gamma_\mu - f_M \sigma_{\mu\nu} q_\nu + i f_S q_\mu \\ A_\mu &= g_A \gamma_\mu \gamma_5 - f_T \sigma_{\mu\nu} q_\nu \gamma_5 + i f_P q_\mu \gamma_5. \end{aligned} \quad (\text{A18})$$

Were we discussing the weak interaction between point-like spin-1/2 fermions, then we would set $g_V = g_A = 1$, and $f_M = f_S = f_T = f_P = 0$. However, in considering nucleons, we recognize that they are not point-like and furthermore they are influenced by the presence of the strong interaction. Thus Eq. (A18) presents the most general form of a vector and axial-vector interaction that is consistent with Lorentz invariance and excludes momentum operators beyond the first power. Here $q_\mu = (p_f - p_i)_\mu$ is the momentum transfer. The coefficients, in principle, could be functions of q^2 but, because of the low four-momentum transfer in beta decay, this q^2 dependence can be neglected and the coefficients are referred to as coupling constants with individual titles: g_V being vector; g_A , axial-vector; f_M , weak magnetic; f_S , induced scalar; f_T , induced tensor and f_P , induced pseudoscalar.

Our aim is to reduce the matrix element $i\bar{u}_f(V_\mu + A_\mu)u_i$, where \bar{u}_f and u_i are Dirac spinors characterising nucleons of momentum \mathbf{p}_f and \mathbf{p}_i , to the nonrelativistic form involving Pauli two-component spinors,

$$\chi_{m_f}^\dagger (V_0 + \mathbf{V} + A_0 + \mathbf{A}) \chi_{m_i}, \quad (\text{A19})$$

by simply multiplying out the Dirac matrices involved and keeping terms to first order in $|\mathbf{p}|/M_N$, and dropping terms in $|\mathbf{p}^2|/M_N^2$ and higher order. This multiplication yields

$$V_0 = g_v + f_s(W_0 - V(r)) \quad (\text{A20})$$

$$\mathbf{V} = \frac{g_v}{2M_N} [\mathbf{p} + i\boldsymbol{\sigma} \times \mathbf{q}] + f_M i\boldsymbol{\sigma} \times \mathbf{q} - f_s \mathbf{q} \quad (\text{A21})$$

$$A_0 = -\frac{g_A}{2M_N} \boldsymbol{\sigma} \cdot \mathbf{p} - f_T \boldsymbol{\sigma} \cdot \mathbf{q} \quad (\text{A22})$$

$$\mathbf{A} = -g_A \boldsymbol{\sigma} + f_T (W_0 - V(r)) \boldsymbol{\sigma}, \quad (\text{A23})$$

where $\mathbf{p} = \mathbf{p}_f + \mathbf{p}_i$ and $\mathbf{q} = \mathbf{p}_f - \mathbf{p}_i$. Note that the large terms of order unity occur in V_0 and \mathbf{A} . Each of the four coupling constants denoted by an f are small and of order $1/M_N$ and, as a consequence, terms in f/M_N have been dropped. Eqs. (A20) to (A23) are the quantities needed in the operators $\hat{T}_{KLS}^M(\hat{\mathbf{r}})$ in Eq. (A17).

4. Reduced matrix elements

All the beta-decay observables [166] can be expressed in terms of the functions $M_K(k_e, k_\nu)$ and $m_K(k_e, k_\nu)$ defined in Eq. (A13). Here we are only interested in the shape-correction function, Eq. (A10), which is a particularly simple combination of these quantities. Before proceeding to evaluate $M_K(k_e, k_\nu)$ and $m_K(k_e, k_\nu)$, we note that the expressions for both differ only in the presence of $F(r)$ in one case and $f(r)$ in the other. For simplicity in what follows, we will only explicitly display formulae incorporating $f(r)$; obviously an equivalent set can be written with $F(r)$.

The operators $\hat{T}_{KLS}^M(\hat{\mathbf{r}})$ are shown in Eq. (A17), but it is tidier if we incorporate the phase, $(-)^{K-L}$ (see Eq. (A13)), into the operator. All the operators (some after rearrangement) can then be expressed as a product of spherical tensors, one in orbital space and one in spin space. So, generically the operators take the form

$$T_{KLS}^M(\mathbf{r}) = f(r)(-)^{K-L} T_{KM}(\Lambda_L \otimes \Sigma_S), \quad (\text{A24})$$

where Λ_L is a spherical tensor in orbital space of multipolarity L , and Σ_S a spherical tensor in spin space⁷. We have introduced notation for a composite spherical tensor obtained from the combination of two other spherical tensors: *viz.*

$$T_{KM}(\Lambda_L \otimes \Sigma_S) = \sum_{M_L M_S} \langle LM_L SM_S | KM \rangle \Lambda_{LM_L} \Sigma_{SM_S}. \quad (\text{A25})$$

The single-particle wave functions from the shell model can also be expressed as products of orbital and spin space functions:

$$|jm\rangle = \sum_{m_l m_s} \langle lm_l \frac{1}{2} m_s | jm \rangle R_{nl}(r) i^l Y_{lm_l}(\hat{\mathbf{r}}) \chi_{m_s}, \quad (\text{A26})$$

where n is the principal quantum number designating the number of nodes in the radial function. Notice the presence of i^l with the spherical harmonics⁸.

The first step in evaluating the reduced matrix element is to factorize it into orbital and spin reduced matrix elements:

$$\begin{aligned} \langle (l_\alpha \frac{1}{2}) j_\alpha \| T_{KLS} \| (l_\beta \frac{1}{2}) j_\beta \rangle = \\ (-)^{K-L} A_{(LS)K} \langle l_\alpha \| f(r) \Lambda_L \| l_\beta \rangle \langle \frac{1}{2} \| \Sigma_S \| \frac{1}{2} \rangle, \end{aligned} \quad (\text{A27})$$

where

$$A_{(LS)K} = \hat{j}_\alpha \hat{K} \hat{j}_\beta \begin{Bmatrix} l_\alpha & \frac{1}{2} & j_\alpha \\ l_\beta & \frac{1}{2} & j_\beta \\ L & S & K \end{Bmatrix}. \quad (\text{A28})$$

Our conventions on reduced matrix elements are those of Edmonds [178]. Next, we need to define two spin matrix elements, denoted S_0 and S_1 and given by

$$\begin{aligned} S_0 &\equiv \langle \frac{1}{2} \| 1 \| \frac{1}{2} \rangle = \sqrt{2} \delta_{S,0} \\ S_1 &\equiv \langle \frac{1}{2} \| \boldsymbol{\sigma} \| \frac{1}{2} \rangle = \sqrt{6} \delta_{S,1}; \end{aligned} \quad (\text{A29})$$

and two orbital matrix elements denoted L_L and $L_{(J1)L}(\mathbf{Q})$. The first is

$$L_L \equiv \langle l_\alpha \| f(r) i^L Y_L(\hat{\mathbf{r}}) \| l_\beta \rangle$$

⁷ Note, the upper case S in Eq. (A24) referring to the multipolarity of the spin operator is not the same as the lower case s in Eq. (A17).

⁸ If one-body density matrix elements (OBDME) are imported from a shell-model calculation into this beta-decay environment, then it is important that these OBDME be computed with similar i^l phases included in the definition of single-particle wave functions.

$$= i^{l_\alpha+L+l_\beta} \frac{\hat{l}_\alpha \hat{L} \hat{l}_\beta}{\sqrt{4\pi}} \begin{pmatrix} l_\alpha & L & l_\beta \\ 0 & 0 & 0 \end{pmatrix} \langle R_\alpha | f(r) | R_\beta \rangle, \quad (\text{A30})$$

where the last factor is the radial integral:

$$\langle R_\alpha | f(r) | R_\beta \rangle \equiv \int_0^\infty R_\alpha(r) f(r) R_\beta(r) r^2 dr. \quad (\text{A31})$$

The second involves derivative operators and requires a little more care. The matrix element is

$$L_{(J_1)L}(\mathbf{Q}) \equiv \langle l_\alpha \parallel f(r) i^J T_L(Y_J \otimes \mathbf{Q}) \parallel l_\beta \rangle, \quad (\text{A32})$$

where \mathbf{Q} is either $\mathbf{p} = \mathbf{p}_f + \mathbf{p}_i$ or $\mathbf{q} = \mathbf{p}_f - \mathbf{p}_i$. Thus we write \mathbf{Q} as $\mathbf{p}_f \pm \mathbf{p}_i$ with the upper sign appropriate for \mathbf{p} and the lower sign for \mathbf{q} . Now \mathbf{Q} is also $-i(\nabla_f \pm \nabla_i)$, where the gradient operator acts on either the initial or final nuclear wave function but not on the integrand, $f(r)$. Thus the interpretation is as follows: $\langle \phi_f | f \mathbf{Q} | \phi_i \rangle = -i \{ \pm \langle \phi_f | f | \nabla \phi_i \rangle - \langle \nabla \phi_f | f | \phi_i \rangle \}$. The result for $L_{(J_1)L}(\mathbf{Q})$ is

$$\begin{aligned} L_{(J_1)L}(\mathbf{Q}) &= i^{l_\alpha+l_\beta+J+1} (-)^{J-L} \frac{\hat{J}}{\sqrt{4\pi}} \times \\ &\left\{ \pm U(l_\beta 1 l_\alpha J; l_\beta + 1 L) \begin{pmatrix} l_\alpha & J & l_\beta + 1 \\ 0 & 0 & 0 \end{pmatrix} \hat{l}_\alpha (l_\beta + 1)^{1/2} \langle R_\alpha | f | \left(\frac{d}{dr} - \frac{l_\beta}{r} \right) R_\beta \rangle \right. \\ &\mp U(l_\beta 1 l_\alpha J; l_\beta - 1 L) \begin{pmatrix} l_\alpha & J & l_\beta - 1 \\ 0 & 0 & 0 \end{pmatrix} \hat{l}_\alpha (l_\beta)^{1/2} \langle R_\alpha | f | \left(\frac{d}{dr} + \frac{l_\beta+1}{r} \right) R_\beta \rangle \\ &- (-)^{J+1-L} U(l_\beta J l_\alpha 1; l_\alpha + 1 L) \begin{pmatrix} l_\alpha + 1 & J & l_\beta \\ 0 & 0 & 0 \end{pmatrix} \hat{l}_\beta (l_\alpha + 1)^{1/2} \langle \left(\frac{d}{dr} - \frac{l_\alpha}{r} \right) R_\alpha | f | R_\beta \rangle \\ &\left. + (-)^{J+1-L} U(l_\beta J l_\alpha 1; l_\alpha - 1 L) \begin{pmatrix} l_\alpha - 1 & J & l_\beta \\ 0 & 0 & 0 \end{pmatrix} \hat{l}_\beta (l_\alpha)^{1/2} \langle \left(\frac{d}{dr} + \frac{l_\alpha+1}{r} \right) R_\alpha | f | R_\beta \rangle \right\}, \quad (\text{A33}) \end{aligned}$$

where the upper sign is used for $\mathbf{Q} = \mathbf{p}$ and the lower sign for $\mathbf{Q} = \mathbf{q}$. The U -coefficient is a recoupling of three angular momenta and is related to a $6j$ -symbol:

$$U(abcd; ef) = (-)^{a+b+c+d} \hat{e} \hat{f} \begin{Bmatrix} a & b & e \\ d & c & f \end{Bmatrix}. \quad (\text{A34})$$

Finally, we are ready to write down the specific reduced matrix elements for all the different hadronic components of the weak interaction, Eqs. (A20) to (A23):

Time-like Vector Current

$$\langle (l_\alpha \frac{1}{2}) j_\alpha \parallel f(r) V_0 i^K Y_K \parallel (l_\beta \frac{1}{2}) j_\beta \rangle = \left(g_V + f_s \left(W_0 + \frac{6}{5} \frac{\alpha Z}{R} \right) \right) A_{(K0)K} L_K S_0. \quad (\text{A35})$$

Space-like Axial Current

$$\langle (l_\alpha \frac{1}{2}) j_\alpha \parallel f(r) \mathbf{A} \cdot i^L \mathbf{Y}_{KL} \parallel (l_\beta \frac{1}{2}) j_\beta \rangle = (-)^{K-L} \left(-g_A + f_T \left(W_0 + \frac{6}{5} \frac{\alpha Z}{R} \right) \right) A_{(L1)K} L_L S_1. \quad (\text{A36})$$

In Eqs. (A35) and (A36), for simplicity we have replaced the function, $V(r)$ (see Eqs. (A20) and (A23)) by the potential due to a uniform charge distribution for small r , with r^2 replaced by its expectation value. In our computations we actually included the function $V(r)$ in the integrand of the appropriate radial integral.

Space-like Vector Current

$$\begin{aligned} \langle (l_\alpha \frac{1}{2}) j_\alpha \parallel f(r) \mathbf{V} \cdot i^L \mathbf{Y}_{KL} \parallel (l_\beta \frac{1}{2}) j_\beta \rangle = \\ (-)^{K-L} \left\{ \frac{g_V}{2M_N} A_{(K0)K} L_{(L1)K}(\mathbf{p}) S_0 - f_s A_{(K0)K} L_{(L1)K}(\mathbf{q}) S_0 \right. \\ \left. - \sqrt{2} \sum_J U(11KL; 1J) \left(\frac{g_V}{2M_N} + f_M \right) A_{(J1)K} L_{(L1)J}(\mathbf{q}) S_1 \right\}. \quad (\text{A37}) \end{aligned}$$

Time-like Axial Current

$$\begin{aligned} \langle (l_\alpha \frac{1}{2}) j_\alpha \parallel f(r) A_0 i^K Y_K \parallel (l_\beta \frac{1}{2}) j_\beta \rangle = \\ \sum_J (-)^{J-K} \frac{\hat{J}}{\hat{K}} \left\{ -\frac{g_A}{2M_N} A_{(J1)K} L_{(K1)J}(\mathbf{p}) S_1 - f_T A_{(J1)K} L_{(K1)J}(\mathbf{q}) S_1 \right\}. \quad (\text{A38}) \end{aligned}$$

5. Numerical Results

The key ingredient for the computation of exact electron wave functions in beta decay is the charge-density distribution of the daughter nucleus. There are various parameterizations available in the literature, of which the following are the most common:

- *Two-parameter Fermi distribution (2pF)*. This charge density distribution,

$$\rho(r) = \frac{\rho_0}{1 + \exp\{(r - c)/a\}}, \quad (\text{A39})$$

has two parameters, c and a , other than its normalization.

- *Three-parameter Fermi distribution (3pF)*. This is an extension of the two-parameter model, which introduces a dimensionless “wine-bottle” parameter, w , that impacts on the small- r behaviour of the density distribution. The functional form is

$$\rho(r) = \frac{\rho_0(1 + wr^2/c^2)}{1 + \exp\{(r - c)/a\}}. \quad (\text{A40})$$

- *Three-parameter Gaussian distribution (3pG)*. This is an alternative three-parameter model with a Gaussian rather than a Fermi distribution:

$$\rho(r) = \frac{\rho_0(1 + wr^2/c^2)}{1 + \exp\{(r^2 - c^2)/a^2\}}. \quad (\text{A41})$$

- *Harmonic-oscillator distribution (HO)*. In light p -shell nuclei, where only s and p orbitals are occupied, a density distribution can be constructed from the harmonic oscillator radial wavefunctions. Its form is

$$\rho(r) = \rho_0(1 + \alpha r^2/b^2) \exp(-r^2/b^2), \quad (\text{A42})$$

where b is the harmonic oscillator length parameter, and α is related to the number of p -shell protons, $\alpha = (Z - 2)/3$. However, in practise both b and α are treated as free parameters and adjusted to fit the elastic-electron scattering data.

These model distributions typically contain two or three parameters. Where possible, the parameters are determined from experimental data on elastic electron scattering, since the measured electron-scattering form factors are just the Fourier transforms of the charge-density distributions. A compilation of charge-density distributions determined from electron scattering is given by De Vries *et al.* [179]. We have assessed these data and selected for each daughter nucleus what we believe to be the ‘best’ value of the rms radius, $\langle r^2 \rangle^{1/2}$, and its probable error. In cases where data are not available on the isotope of interest, we have examined the nearest isotope that is available and applied a modest isotope shift to its value of $\langle r^2 \rangle^{1/2}$. Our final selected values are listed in Table X. We also list the percentage uncertainty in the exact value of f due solely to the uncertainty in $\langle r^2 \rangle^{1/2}$. Clearly, the uncertainty in the charge-density distribution is not a factor in the determination of f to 0.1% accuracy.

Before the final evaluation of the statistical rate function, f , there are two further corrections to consider: for screening and recoil. To accommodate these corrections and to

TABLE X: Charge-density distributions from elastic electron-scattering data [179]. The radius parameter, in some cases, has been adjusted to reproduce $\langle r^2 \rangle^{1/2}$. Parameters, c and a , are in fm units, parameter w is dimensionless.

Daughter Nucleus	$\langle r^2 \rangle^{1/2}$ fm	Model ^b	c	a	w	Δf^a %
$T_z = -1$:						
¹⁰ B	2.45(10)	HO	1.709 ^c	0.837 ^d		0.001
¹⁴ N	2.52(2)	3pF	2.572	0.5052	-0.180	0.000
¹⁸ F	2.90(3)	2pF	2.574	0.567		0.001
²² Na	2.95(5)	2pF	2.750	0.549		0.001
²⁶ Al	3.03(2)	2pF	2.791	0.569		0.001
³⁰ P	3.18(3)	3pF	3.350	0.582	-0.173	0.002
³⁴ Cl	3.39(2)	3pF	3.479	0.599	-0.100	0.001
³⁸ K	3.41(4)	3pF	3.738	0.585	-0.201	0.004
⁴² Sc	3.50(5)	3pF	3.794	0.586	-0.161	0.004
$T_z = 0$:						
²⁶ Mg	3.06(5)	2pF	3.049	0.523		0.002
³⁴ S	3.29(1)	3pG	2.810	2.191	0.160	0.001
³⁸ Ar	3.36(5)	2pF	3.590	0.507		0.004
⁴² Ca	3.48(3)	3pF	3.765	0.586	-0.161	0.002
⁴⁶ Ti	3.61(3)	2pF	3.711	0.588		0.003
⁵⁰ Cr	3.66(4)	2pF	3.868	0.566		0.004
⁵⁴ Fe	3.69(2)	3pG	3.541	2.270	0.403	0.003
⁶² Zn	3.90(2)	3pG	3.570	2.465	0.342	0.005
⁶⁶ Ge	4.04(4)	2pF	4.398	0.585		0.011
⁷⁰ Se	4.07(5)	2pF	4.442	0.585		0.011
⁷⁴ Kr	4.10(5)	2pF	4.489	0.585		0.013

^aPercentage uncertainty in f due to the uncertainty in $\langle r^2 \rangle^{1/2}$.

^bSee Eqs.(A39) to (A42).

^cThis is parameter, b , of Eq. (A42) in fm units.

^dThis is the dimensionless parameter, α , of Eq. (A42).

remove – as is customary – the leading matrix element from the definition of f , we rewrite f as follows:

$$f = \xi R(W_0) \int_1^{W_0} pW(W_0 - W)^2 F_0 L_0 C(Z, W) Q(Z, W) dW. \quad (\text{A43})$$

Comparison with Eqs. (A1) and (A3) reveals three new factors, $Q(Z, W)$, $R(W_0)$ and ξ . We will deal with them in that order.

The calculation of the Fermi function presented so far makes no allowance for the screening of the atomic electrons. Rose [180] was the first to find a simple analytic prescription to obtain the Fermi function for a screened field from the Fermi function for the corresponding unscreened field. That prescription is to incorporate a correction factor into the integrand for f : *viz*

$$Q(Z, W) = \frac{\tilde{p}\tilde{W} F(Z, \tilde{W})}{pW F(Z, W)}, \quad (\text{A44})$$

where $\tilde{W} = W - V_0$, $\tilde{p} = (\tilde{W}^2 - 1)^{1/2}$ and $V_0 = N(\tilde{Z})\alpha^2\tilde{Z}^{4/3}$, with \tilde{Z} being the electronic charge of the parent atom and $N(\tilde{Z})$ being a weak function of \tilde{Z} , which varies from $N = 1.42$ at $\tilde{Z} = 8$ to $N = 1.56$ at $\tilde{Z} = 29$ (see Matese and Johnson [181]). Since the factor $Q(Z, W)$ yields a correction to f of order $\sim 0.2\%$, we only need Rose's screening correction to be accurate to within 50% of its central value in order to assure us an accuracy in f of 0.1%. Matese and Johnson [181] have tested the Rose formula by comparing it with numerical solutions of the Dirac equation for a self-consistent Hartree-Fock-Slater potential. They conclude that $Q(Z, W)$ has an accuracy of four significant figures or better for all energies except the very lowest in positron emitters. Since we integrate $Q(Z, W)$ over the whole beta spectrum, which actually de-emphasizes the lowest positron energies, we conclude that the Rose formula has far more than sufficient accuracy for our purpose.

The second new factor in Eq. (A43) is $R(W_0)$, which is the correction for recoil: it recognizes that the daughter nucleus is not at rest but has a small amount of recoiling kinetic energy. As a result, the leptons' maximum energy is actually slightly less than W_0 . The recoil correction [166] is

$$R(W_0) = 1 - \frac{3W_0}{2M_A}, \quad (\text{A45})$$

where M_A is the average of the initial and final nuclear masses. For use in eq. (A45), M_A must, like W_0 , be expressed in electron rest-mass units. The resulting correction is very small, being of order 0.02% for the superallowed beta decays from $A = 10$ to $A = 74$.

Lastly, for allowed transitions it is customary to remove the leading matrix element from the definition of f . Thus, we have introduced ξ in Eq. (A43), where $\xi = 1/|M_F|^2$ for superallowed Fermi transitions, M_F being the Fermi matrix element. For pure Gamow-Teller transitions $\xi = 1/|M_{GT}|^2$, with M_{GT} being the Gamow-Teller matrix element.

In Table XI we list both the values of f_{stat} , Eq. (A2), and the exact values of f for cases of interest in superallowed beta decay. The relevant Q_{EC} value is listed as well. For the exact

TABLE XI: Comparison of statistical rate functions, f_{stat} , f_{approx} and the exact value, f .

Parent	Q_{EC} keV	W_0	f_{stat}	f	Δf_{stat}^a %
$T_z = -1$:					
^{10}C	1907.9	2.7336	2.29484	2.30089	-0.26
^{14}O	2831.0	4.5400	42.6147	42.7485	-0.31
^{18}Ne	3402.0	5.6575	133.867	134.484	-0.46
^{22}Mg	4124.6	7.0716	415.826	418.440	-0.62
^{26}Si	4836.9	8.4656	1014.75	1023.28	-0.83
^{30}S	5459.5	9.6840	1945.49	1967.05	-1.10
^{34}Ar	6062.8	10.8647	3366.22	3414.21	-1.41
^{38}Ca	6614.2	11.9437	5247.54	5338.46	-1.70
^{42}Ti	7000.9	12.7004	6904.47	7042.83	-1.96
$T_z = 0$:					
^{26m}Al	4232.5	7.2828	474.691	478.176	-0.73
^{34}Cl	5491.8	9.7472	1971.95	1996.39	-1.22
^{38m}K	6044.4	10.8286	3248.45	3298.10	-1.51
^{42}Sc	6425.7	11.5748	4391.71	4470.41	-1.76
^{46}V	7050.7	12.7979	7044.04	7199.96	-2.17
^{50}Mn	7632.5	13.9364	10456.3	10731.6	-2.57
^{54}Co	8242.7	15.1305	15281.4	15750.1	-2.98
^{62}Ga	9171.0	16.9472	25187.9	26247.6	-4.04
^{66}As	9550.0	17.6889	30146.4	31613.7	-4.64
^{70}Br	9970.0	18.5108	36605.4	38602.2	-5.17
^{74}Rb	10416.5	19.3846	44606.1	47277.8	-5.65

$$^a \Delta f_{\text{stat}} = 100 * (f_{\text{stat}} - f) / f$$

calculations, we imported one-body density matrix elements, OBDME, from a shell-model code. For each case we performed several shell-model calculations for various sets of effective interactions and model spaces. We used, in fact, the same wave functions that we used [158] to compute the nuclear-structure corrections δ_C and δ_{NS} . Thus our f calculations can be considered to be entirely consistent with the calculation of the nuclear-structure-dependent corrections. The f calculation, however, is not very sensitive to the shell-model inputs. In light nuclei, different shell-model OBDME gave changes in f at the 0.01% level, increasing to around 0.1% in $A = 74$, our heaviest-mass case. Where we have more than one shell-model calculation for a given nucleus, we have averaged the f values for the entry in Table XI.

-
- [1] I.S. Towner and J.C. Hardy, *J. Phys. G: Nucl. Part. Phys.*, **29**, 197 (2003).
 - [2] A. Sher *et al.*, *Phys. Rev. Lett.* **91**, 261802 (2003).
 - [3] I.S. Towner and J.C. Hardy, *Nucl. Phys.* **A205**, 33 (1973).
 - [4] J.C. Hardy and I.S. Towner, *Nucl. Phys.* **A254**, 221 (1975).
 - [5] V.T. Koslowsky, E. Hagberg, J.C. Hardy, H. Schmeing, R.E. Azuma and I.S. Towner, in *Proc. 7th Int. Conf. on atomic masses and fundamental constants, Darmstadt-Seeheim*, ed. O. Klepper (T.H. Darmstadt, 1984) p. 572
 - [6] J.C. Hardy, I.S. Towner, V.T. Koslowsky, E. Hagberg and H. Schmeing, *Nucl. Phys.* **A509**, 429 (1990).
 - [7] S. Eidelman *et al*, *Phys. Lett.* **B592**, 1 (2004).
 - [8] E.G. Adelberger, M.M. Hindi, C.D. Hoyle, H.E. Swanson, R.D. Von Lintig and W.C. Haxton, *Phys. Rev. C* **27**, 2833 (1983); this reference replaces the result reported in E.G. Adelberger, C.D. Hoyle, H.E. Swanson and R.D. Von Lintig, *Phys. Rev. Lett.* **46**, 695 (1981).
 - [9] F. Ajzenberg-Selove, *Nucl. Phys.* **A490**, 1 (1988).
 - [10] F. Ajzenberg-Selove, *Nucl. Phys.* **A523**, 1 (1991).
 - [11] A.M. Aldridge, K.W. Kemper and H.S. Plendl, *Phys. Lett.* **30B**, 165 (1969)
 - [12] D.E. Alburger and D.H. Wilkinson, *Phys. Lett.* **32B**, 190 (1970).
 - [13] D.E. Alburger, *Phys. Rev. C* **5**, 274 (1972).
 - [14] D.E. Alburger and F.P. Calaprice, *Phys. Rev. C* **12**, 1690 (1975).
 - [15] D.E. Alburger and D.H. Wilkinson, *Phys. Rev. C* **15**, 2174 (1977); this reference replaces the

- ^{46}V half-life from [149].
- [16] D.E. Alburger, Phys. Rev. C **18**, 1875 (1978).
 - [17] P.F.A. Alkemade, C. Alderliesten, P. De Wit and C. Van der Leun, Nucl. Instr and Meth. **197**, 383 (1982).
 - [18] A. Antilla, M. Bister and E. Arminen, Z. Phys. **234**, 455 (1970).
 - [19] E. Aslanides, F. Jundt and A. Gallmann, Nucl. Phys. **A152**, 251 (1970).
 - [20] G. Audi, A.H. Wapstra and C. Thibault, Nucl. Phys. **A729**, 327 (2003).
 - [21] G. Azuelos, J.E. Crawford and J.E. Kitching, Phys. Rev. C **9**, 1213 (1974).
 - [22] G. Azuelos and J.E. Kitching, Phys. Rev. C **12**, 563 (1975).
 - [23] R.K. Barden, C.A. Barnes, W.A. Fowler and P.G. Seeger, Phys. Rev. **127**, 583 (1962)
 - [24] F.J. Bartis, Phys. Rev. **132**, 1763 (1963).
 - [25] P.H. Barker, N. Drysdale and W.R. Phillips, Proc. Phys. Soc **91**, 587 (1967).
 - [26] P.H. Barker, C.J. Scofield, R.J. Petty, J.M. Freeman, S.D. Hoath, W.E. Burcham and G.T.A. Squier, Nucl. Phys. **A275**, 37 (1977); the same result also appears in G.T.A. Squier, W.E. Burcham, S.D. Hoath, J.M. Freeman, P.H. Barker and R.J. Petty, Phys. Lett. **65B**, 122 (1976).
 - [27] P.H. Barker and J.A. Nolen, Proc. Int. Conf. on Nucl. Structure, Tokyo, Japan, 1977.
 - [28] P.H. Barker, R.E. White, H. Naylor and N.S. Wyatt, Nucl. Phys. **A279**, 199 (1977).
 - [29] P.H. Barker and R.E. White, Phys. Rev. C **29**, 1530 (1984).
 - [30] P.H. Barker and S.M. Ferguson, Phys. Rev. C **38**, 1936 (1988).
 - [31] S.C. Baker, M.J. Brown and P.H. Barker, Phys. Rev. C **40**, 940 (1989).
 - [32] P.H. Barker and G.D. Leonard, Phys. Rev. C **41**, 246 (1990).
 - [33] P.H. Barker and P.A. Amundsen, Phys. Rev. C **58**, 2571 (1998); this reference updates the ^{10}C Q_{EC} -value from [31]; its value for the ^{14}O Q_{EC} -value was later withdrawn in [141].
 - [34] P.H. Barker and M.S. Wu, Phys. Rev C **62**, 054302 (2000).
 - [35] G.C. Ball, S. Bishop, J.A. Behr, G.C. Boisvert, P. Bricault, J. Cerny, J.M. D'Auria, M. Dombisky, J.C. Hardy, V. Iacob, J.R. Leslie, T. Lindner, J.A. Macdonald, H.-B. Mak, D.M. Moltz, J. Powell, G. Savard and I.S. Towner, Phys. Rev. Lett. **86**, 1454 (2001).
 - [36] P.H. Barker, I.C. Barnett, G.J. Baxter and A.P. Byrne, Phys. Rev. C **70**, 024302 (2004).
 - [37] G.C. Ball **et al**, to be published.
 - [38] E. Beck and H. Daniel, Z. Phys. **216**, 229 (1968).

- [39] J.A. Becker, R.A. Chalmers, B.A. Watson and D.H. Wilkinson, Nucl. Instr. Meth. **155**, 211 (1978).
- [40] F.J. Bergmeister, K.P. Lieb, K. Pampus and M. Uhrmacher, Z. Phys. **A320**, 693 (1985).
- [41] S. Bishop et al., Phys. Rev. Lett. **90**, 162501 (2003).
- [42] B. Blank, Eur. Phys. J. **A15**, 121 (2002).
- [43] B. Blank, G. Savard, J. Doring, A. Blazhev, G. Canchel, M. Chartier, D. Henderson, Z. Janas, R. Kirchner, I. Mukha, E. Roeckl, K. Schmidt, and J. Zylicz, Phys. Rev. C **69**, 015502 (2004).
- [44] K. Blaum, G. Audi, D. Beck, G. Bollen, C. Guenaut, P. Delahaye, F. Herfurth, A. Kellerbauer, H.-J. Kluge, D. Lunney, D. Rodriguez, S. Schwarz, L. Schweikhard, C. Weber and C. Yazidjian, Nucl. Phys. **A**, to be published.
- [45] R.O. Bondelid and J.W. Butler, Nucl. Phys. **53**, 618 (1964).
- [46] S.A. Brindhaban and P.H. Barker, Phys. Rev. C **49**, 2401 (1994); reference replaces earlier conference proceedings from the same laboratory.
- [47] J.W. Butler and R.O. Bondelid, Phys. Rev. **121**, 1770 (1961).
- [48] W.E. Burcham and G.T.A. Squier, Nucl. Instr. And Meth. **164**, 533 (1979).
- [49] R.H. Burch, C.A. Gagliardi and R.E. Tribble, Phys. Rev. C **38**, 1365 (1988).
- [50] G. Canchel, B. Blank, M. Chartier, F. Delalee, P. Dendooven, C. Dossat, J. Giovinazzo, J. Huikari, A.S. Lalleman, M.J. Lopez Jimenez, V. Madec, J.L. Pedroza, H. Penttila and J.C. Thomas, Eur. Phys. J. **A**, to be published.
- [51] N.M. Chaudri, Fizika **16**, 297 (1984).
- [52] G.J. Clark, J.M. Freeman, D.C. Robinson, J.S. Ryder, W.E. Burcham and G.T.A. Squier, Nucl. Phys. **A215**, 429 (1973); this reference replaces the half-life value in G.J. Clark, J.M. Freeman, D.C. Robinson, J.S. Ryder, W.E. Burcham and G.T.A. Squier, Phys. Lett **35B**, 503 (1971).
- [53] C.N. Davids, C.A. Gagliardi, M.J. Murphy and E.B. Norman, Phys. Rev. C **19**, 1463 (1979).
- [54] C.N. Davids, in “Atomic masses and fundamental constants 6”, eds. J.A. Nolen and W. Benenson (Plenum, New York, 1980) p. 419.
- [55] W.W. Daehnick and R.D. Rosa, Phys. Rev. C **31**, 1499 (1985).
- [56] P. De Wit and C. Van der Leun, Phys. Lett. **30B**, 639 (1969).
- [57] R.M. DelVecchio and W.W. Daehnick, Phys. Rev. C **17**, 1809 (1978).

- [58] M.A. van Driel, H. Klijnman, G.A.P. Engelbertink, H.H. Eggebhuisen and J.A.J. Hermans, Nucl. Phys. **A240**, 98 (1975).
- [59] L.G. Earwaker, J.G. Jenkin and E.W. Titterton, Nature **195**, 271 (1962).
- [60] P.M. Endt, Nucl. Phys. **A521**, 1 (1990).
- [61] P.M. Endt, Nucl. Phys. **A633**, 1 (1998).
- [62] G. Frick, A. Gallmann, D.E. Alburger, D.H. Wilkinson and J.P. Coffin, Phys. Rev. **132**, 2169 (1963).
- [63] J.M. Freeman, G. Murray and W.E. Burcham, Phys.Lett. **17**, 317 (1965).
- [64] J.M. Freeman, J.G. Jenkin, G. Murray, D.C. Robinson and W.E. Burcham, Nucl. Phys. **A132**, 593 (1969); this reference replaces the half-life values in J.M. Freeman, J.H. Montague, G. Murray, R.E. White and W.E. Burcham, Nucl. Phys. **69**, 433 (1965) and J.M. Freeman, J.G. Jenkin, G. Murray and W.E. Burcham, Phys. Rev. Lett. **16**, 959 (1966).
- [65] J.M. Freeman, R.J. Petty, S.D. Hoath, G.T.A. Squier and W.E. Burcham, Phys. Lett **53B**, 439 (1975).
- [66] B.K. Fujikawa, S.J. Asztalos, R.M. Clark, M.A. Deleplanque-Stephens, P. Fallon, S.J. Freeman, J.P. Greene, I.-Y. Lee, L.J. Lising, A.O. Macchiavelli, R.W. MacLeod, J.C. Reich, M.A. Rowe, S.-Q. Shang, F.S. Stephens and E.G. Wasserman, Phys. Lett. **B449**, 6 (1999).
- [67] A Gallmann, E. Aslanides, F. Jundt and E. Jacobs, Phys. Rev. **186**, 1160 (1969).
- [68] M. Gaelens, J. Andrzejewski, J. Camps, P. Decrock, M. Huyse, K. Kruglov, W.F. Mueller, A. Piechaczek, N. Severijns, J. Szerypo, G. Vancraeynest, P. Van Duppen and J. Wauters, Eur. Phys. J. **A11**, 413 (2001).
- [69] H.J. Gils, D. Flothmann, R. Loehken and W. Wiesner, Nucl. Instr. and Meth. **105**, 179 (1972).
- [70] D.R. Goosman and D.E. Alburger, Phys. Rev. C **5**, 1893 (1972); the branching-ratio upper limit set in this reference is considered to replace the much higher value reported by D.R. Brown, S.M. Ferguson and D.H. Wilkinson, Nucl. Phys. **A135**, 159 (1969).
- [71] G.I. Harris and A.K. Hyder, Phys. Rev. **157**, 958 (1967).
- [72] M. Hagen, K.H. Maier and R. Michaelsen, Phys. Lett. **26B**, 432 (1968).
- [73] J.C. Hardy and D.E. Alburger, Phys. Lett. **B42**, 341 (1972).
- [74] J.C. Hardy, H. Schmeing, J.S. Geiger and R.L. Graham, Nucl. Phys. **A223**, 157 (1974); this reference replaces results in J.C. Hardy, H. Schmeing, J.S. Geiger, R.L. Graham and I.S.

- Towner, Phys. Rev. Lett. **29**, 1027 (1972).
- [75] J.C. Hardy, H.R. Andrews, J.S. Geiger, R.L. Graham, J.A. Macdonald and H. Schmeing, Phys. Rev. Lett. **33**, 1647 (1974).
- [76] J.C. Hardy, H. Schmeing, W. Benenson, G.M. Crawley, E. Kashy and H. Nann, Phys. Rev. C **9**, 252 (1974).
- [77] J.C. Hardy, G.C. Ball, J.S. Geiger, R.L. Graham, J.A. Macdonald and H. Schmeing, Phys. Rev. Lett. **33**, 320 (1974); the value for the ^{46}V Q_{EC} -value from this reference was later withdrawn by J.C. Hardy and I.S. Towner, in “Atomic masses and fundamental constants 5”, eds. J.H. Sanders and A.H. Wapstra (Plenum, New York, 1976) p 66.
- [78] J.C. Hardy, H. Schmeing, J.S. Geiger and R.L. Graham, Nucl. Phys. **A246**, 61 (1975); this reference replaces results in J.C. Hardy, H. Schmeing, J.S. Geiger, R.L. Graham and I.S. Towner, Phys. Rev. Lett. **29**, 1027 (1972).
- [79] E. Hagberg, V.T. Koslowsky, J.C. Hardy, I.S. Towner, J.G. Hykawy, G. Savard and T. Shinozuka, Phys. Rev. Lett. **73**, 396 (1994); uncertainties on the Gamow-Teller decays observed from ^{46}V and ^{50}Mn did not appear in this reference but have been derived from the original data and added here.
- [80] P.D. Harty, N.S. Bowden, P.H. Barker and P.A. Amundsen, Phys. Rev. C **58**, 821 (1998).
- [81] J.C. Hardy and I.S. Towner, Phys. Rev. Lett. **88**, 252501 (2002).
- [82] J.C. Hardy, V.E. Iacob, M. Sanchez-Vega, R.G. Neilson, A. Azhari, C.A. Gagliardi, V.E. Mayes, X. Tang, L. Trache and R.E. Tribble, Phys. Rev. Lett. **91**, 082501 (2003).
- [83] D.L. Hendrie and J.B. Gerhart, Phys. Rev. **121**, 846 (1961).
- [84] A.M. Hernandez and W.W. Daehnick, Phys. Rev. C **24**, 2235 (1981).
- [85] A.M. Hernandez and W.W. Daehnick, Phys. Rev. C **25**, 2957 (1982).
- [86] F. Herfurth et al, Eur. Phys. J. **A15**, 17 (2002).
- [87] I. Hofmann, Acta Phys. Aust. **18**, 309 (1964).
- [88] S.D. Hoath, R.J. Petty, J.M. Freeman, G.T.A. Squier and W.E. Burcham, Phys. Lett. **51B**, 345 (1974).
- [89] P. Hungerford and H.H. Schmidt, Nucl. Instr. and Meth. **192**, 609 (1982).
- [90] B.C. Hyman, V.E. Iacob, A. Azhari, C.A. Gagliardi, J.C. Hardy, V.E. Mayes, R.G. Neilson, M. Sanchez-Vega, X. Tang, L. Trache and R.E. Tribble, Phys. Rev. C **68**, 015501 (2003).
- [91] V.E. Iacob, E. Mayes, J.C. Hardy, R.G. Neilson, M. Sanchez-Vega, A. Azhari, C.A. Gagliardi,

- L. Trache and R.E. Tribble, *Bul. Am. Phys. Soc.* **48**, 34 (2003).
- [92] P.D. Ingalls, J.C. Overley and H.S. Wilson, *Nucl. Phys.* **A293**, 117 (1977).
- [93] M.A. Islam, T.J. Kennett, S.A. Kerr and W.V. Prestwich, *Can. J. Phys.* **58**, 168 (1980).
- [94] J. Jaenecke, *Z. Naturf.* **15a**, 593 (1960).
- [95] A.N. James, F.J. Sharpey-Schafer, A.M. Al-Naser, A.H. Behbehani, C.J. Lister, P.J. Nolan, P.H. Barker and W.E. Burcham, *J. Phys. G* **4**, 579 (1978).
- [96] R.W. Kavanagh, A. Gallmann, E. Aslanides, F. Jundt and E. Jacobs, *Phys. Rev.* **175**, 1426 (1968).
- [97] R.W. Kavanagh, *Nucl. Phys* **A129**, 172 (1969).
- [98] A. Kellerbauer, G. Audi, D. Beck, K. Blaum, G. Bollen, B.A. Brown, P. Delahaye, C. Guenaut, F. Herfurth, H.-J. Kluge, D. Lunney, S. Schwarz, L. Schweikhard and C. Yazidjian, *Phys. Rev. Lett.*, **93**, 072502 (2004).
- [99] S.W. Kikstra, C. van der Leun, S. Raman, E.T. Journey and I.S. Towner, *Nucl. Phys.* **A496**, 429 (1989).
- [100] S.W. Kikstra, Z. Guo, C. Van der Leun, P.M. Endt, S. Raman, Walkiewicz, J.W. Starner, E.T. Journey and I.S. Towner, *Nucl. Phys.* **A529**, 39 (1991).
- [101] V.T. Koslowsky, E. Hagberg, J.C. Hardy, R.E. Azuma, E.T.H. Clifford, H.C. Evans, H. Schmeing, U.J. Schrewe and K.S. Sharma, *Nucl. Phys.* **A405**, 29 (1983).
- [102] V.T. Koslowsky, J.C. Hardy, E. Hagberg, R.E. Azuma, G.C. Ball, E.T.H. Clifford, W.G. Davies, H. Schmeing, U.J. Schrewe and K.S. Sharma, *Nucl. Phys.* **A472**, 419 (1987); the ^{14}O - $^{26}\text{Al}^m$ Q_{EC} -value-difference result reported in this reference replaces an earlier value given in V.T. Koslowsky, J.C. Hardy, R.E. Azuma, G.C. Ball, E.T.H. Clifford, W.G. Davies, E. Hagberg, H. Schmeing, U.J. Schrewe and K.S. Sharma, *Phys. Lett.* **119B**, 57 (1982).
- [103] V.T. Koslowsky, E. Hagberg, J.C. Hardy, G. Savard, H. Schmeing, K.S. Sharma and X.J. Sun, *Nucl.Instr.and Meth.* **A401**, 289 (1997).
- [104] V.T. Koslowsky, E. Hagberg, J.C. Hardy, H. Schmeing and I.S. Towner, *Nucl. Phys.* **A624**, 293 (1997).
- [105] M.A. Kroupa, S.J. Freeman, P.H. Barker and S.M. Ferguson, *Nucl. Instr. And Meth. in Phys. Res.* **A310**, 649 (1991).
- [106] S. Lin, S.A. Brindhaban and P.H. Barker, *Phys. Rev. C* **49**, 3098 (1994).
- [107] P.V. Magnus, E.G. Adelberger and A. Garcia, *Phys. Rev. C* **49**, R1755 (1994).

- [108] W.R. McMurray, P. Van der Merwe and I.J. Van Heerden, Nucl. Phys. **A92**, 401 (1967).
- [109] R.G. Miller and R.W. Kavanagh, Nucl. Phys. **A94**, 261 (1967).
- [110] C.E. Moss, C. Detraz and C.S. Zaidins, Nucl. Phys. **A174**, 408 (1971).
- [111] M. Mukherjee, A. Kellerbauer, D. Beck, K. Blaum, G. Bollen, F. Carrel, P. Delahaye, J. Dilling, S. George, C. Guenaut, F. Herfurth, A. Herlert, H.-J. Kluge, U. Koster, D. Lunney, S. Schwarz, L. Schweikhard and C. Yazidjian, Phys. Rev. Lett. **93**, 150801 (2004).
- [112] Y. Nagai, K. Kunihiro, T. Toriyama, S. Harada, Y. Torii, A. Yoshida, T. Nomura, J. Tanaka and T. Shinozuka, Phys. Rev. C **43**, R9 (1991).
- [113] F.M. Nichols, N. Lawley, I.G. Main, M.F. Thomas and P.J. Twin, Nucl. Phys. **A124**, 97 (1969).
- [114] J.A. Nolen, G. Hamilton, E. Kashy and I.D. Proctor, Nucl. Instr. and Meth. **115**, 189 (1974).
- [115] M.Oinonen *et al*, Phys. Lett. **B511**, 145 (2001).
- [116] R.A. Padock, Phys. Rev. C **5**, 485 (1972).
- [117] A. Piechaczek, E.F. Zganjar, G.C. Ball, P. Bricault, J.M. D'Auria, J.C. Hardy, D.F. Hodgson, V. Iacob, P Klages, W.D. Kulp, J.R. Leslie, M. Lipoglavsek, J.A. Macdonald, H.-B. Mak, D.M. Moltz, G. Savard, J. von Schwarzenberg, C.E. Svensson, I.S. Towner and J.L. Wood, Phys. Rev. C **67**, 051305(R) (2003); the branching-ratio results from this measurement are considered to replace the contradictory upper limit set in an earlier less-precise measurement[115].
- [118] F.W. Prosser, G.U. Din and D.D. Tolbert, Phys. Rev. **157**, 779 (1967).
- [119] W.V. Prestwich and T.J. Kennett, Can. J. Phys. **68**, 261 (1990); erratum **68**, 1352 (1990).
- [120] S. Raman, E.T. Journey, D.A. Outlaw and I.S. Towner, Phys. Rev. C **27**, 1188 (1983).
- [121] J.P.L. Reinecke, F.B. Waanders, P. Oberholtzer, P.J.C. Janse van Rensburg, J.A. Cilliers, J.J.A. Smit, M.A. Meyer and P.M. Endt, Nucl. Phys. **A435**, 333 (1985).
- [122] M.L. Roush, L.A. West and J.B. Marion, Nucl. Phys. **A147**, 235 (1970).
- [123] D.C. Robinson, J.M. Freeman and T.T. Thwaites, Nucl. Phys. **A181**, 645 (1972); this reference replaces the ^{10}C branching ratio from J.M. Freeman, J.G. Jenkin and G. Murray, Nucl. Phys. **A124**, 393 (1969).
- [124] D.C. Robinson and P.H. Barker, Nucl. Phys. **A225**, 109 (1974).
- [125] C. Rolfs, W.S. Rodney, S. Durrance and H. Winkler, Nucl. Phys. **A240**, 221 (1975).
- [126] J.S. Ryder, G.J. Clark, J.E. Draper, J.M. Freeman, W.E. Burcham and G.T.A. Squier, Phys.

- Lett **43B**, 30 (1973).
- [127] A Rytz, At. Data and Nucl. Data Tables **47**, 205 (1991).
- [128] A.M. Sandorfi, C.J. Lister, D.E. Alburger and E.K. Warburton, Phys. Rev. C **22**, 2213 (1980).
- [129] G. Savard, A. Galindo-Uribarri, E. Hagberg, J.C. Hardy, V.T. Koslowsky, D.C. Radford and I.S. Towner, Phys. Rev. Lett. **74**, 1521 (1995).
- [130] G. Savard, J.A. Clark, F. Buchinger, J.E. Crawford, S. Gulick, J.C. Hardy, A.A. Hecht, V.E. Jacob, J.K.P. Lee, A.F. Levand, B.F. Lundgren, N.D. Scielzo, K.S. Sharma, I. Tanihata, I.S. Towner, W. Trimble, J.C. Wang, Y. Wang and Z. Zhou, Phys. Rev. C **70**, 042501(R) (2004).
- [131] R.J. Scott, R.P. Rassool, M.N. Thompson and D.V. Webb, Nucl. Instr. and Meth. in Phys. Res. **A**, to be published.
- [132] J.C. Sens, A. Pape and R. Armbruster, Nucl. Phys. **A199**, 241 (1973).
- [133] K.K. Seth, A. Saha, W. Benenson, W.A. Lanford, H. Nann and B.H. Wildenthal, Phys. Rev. Lett. **33**, 233 (1974).
- [134] D. Seweryniak, to be published.
- [135] R. Sherr, J.B. Gerhart, H. Horie and W.F. Hornyak, Phys. Rev. **100**, 945 (1955).
- [136] G.S. Sidhu and J.B. Gerhart, Phys. Rev. **148**, 1024 (1963).
- [137] J. Singh, Indian J. Pure Appl. Phys. **10**, 289 (1972).
- [138] G.T.A. Squier, W.E. Burcham, J.M. Freeman, R.J. Petty, S.D. Hoath and J.S. Ryder, Nucl. Phys **A242**, 62 (1975).
- [139] G.T.A. Squier, W.E. Burcham, S.D. Hoath, J.M. Freeman, P.H. Barker and R.J. Petty, Phys. Lett. **65B**, 122 (1976).
- [140] D.R. Tilley, H.R. Weller, C.M. Cheves and R.M. Chasteler, Nucl. Phys. **A595**, 1 (1995).
- [141] N.R. Tolich, P.H. Barker, P.D. Harty and P.A. Amundsen, Phys. Rev. C **67**, 035503 (2003).
- [142] H. Vonach, P. Glaessel, E. Huenges, P. Maier-Komor, H. Roesler, H.J. Scheerer, H. Paul and D. Semrad, Nucl. Phys. **A278**, 189 (1977).
- [143] F.B. Waanders, J.P.L. Reinecke, H.N. Jacobs, J.J.A. Smit, M.A. Meyer and P.M. Endt, Nucl. Phys. **A411**, 81 (1983).
- [144] T.A. Walkiewicz, S. Raman, E.T. Journey, J.W. Starner and J.E. Lynn, Phys. Rev. C **45**, 1597 (1992).
- [145] H. Wenninger, J. Stiewe and H. Leutz, Nucl. Phys. **A109**, 561 (1968).

- [146] R.E. White and H. Naylor, Nucl. Phys. **A276**, 333 (1977).
- [147] R.E. White, H. Naylor, P.H. Barker, D.M.J. Lovelock and R.M. Smythe, Phys. Lett. **105B**, 116 (1981).
- [148] R.E. White, P.H. Barker and D.M.J. Lovelock, Metrologia **21**, 193 (1985).
- [149] D.H. Wilkinson and D.E. Alburger, Phys. Rev. C **13**, 2517 (1976).
- [150] D.H. Wilkinson, A. Gallmann and D.E. Alburger, Phys. Rev. C **18**, 401 (1978).
- [151] H.S. Wilson, R.W. Kavanagh and F.M. Mann, Phys. Rev. C **22**, 1696 (1980).
- [152] J. Zioni, A.A. Jaffe, E. Friedman, N. Haik, R. Schectman and D. Nir, Nucl. Phys. **A181**, 465 (1972).
- [153] F. Zijderhand, R.C. Markus and C. van der Leun, Nucl. Phys. **A466**, 280 (1987).
- [154] W. Bambynek, H. Behrens, M.H. Chen, B. Crasemann, M.L. Fitzpatrick, K.W.D. Ledingham, H. Genz, M. Mutterer and R.L. Intemann, Rev. Mod. Phys. **49**, 77 (1977).
- [155] R.B. Firestone, *Table of Isotopes, Eighth Edition*, (Wiley, New York, 1996).
- [156] A. Sirlin, Phys. Rev. D **35**, 3423 (1987); A. Sirlin and R. Zucchini, Phys. Rev. Lett. **57**, 1994 (1986).
- [157] W. Jaus and G. Rasche, Phys. Rev. D **35**, 3420 (1987).
- [158] I.S. Towner and J.C. Hardy, Phys. Rev. C **66**, 035501 (2002).
- [159] W.E. Ormand and B.A. Brown, Phys. Rev. C **52**, 2455 (1995); W.E. Ormand and B.A. Brown, Phys. Rev. Lett. **62**, 866 (1989); W.E. Ormand and B.A. Brown, Nucl. Phys. **A440**, 274 (1985).
- [160] H. Sagawa, N. Van Giai and T. Suzuki, Phys. Rev. C **53**, 2163 (1996).
- [161] F.C. Barker, Nucl. Phys. **A537**, 134 (1992).
- [162] D.H. Wilkinson, Nucl. Instr. and Meth. A **488**, 654 (2002); D.H. Wilkinson, Nucl. Instr. and Meth. A **526**, 386 (2004).
- [163] W.J. Marciano and A. Sirlin, Phys. Rev. Lett. **56**, 22 (1986).
- [164] A. Sirlin, in *Precision Tests of the Standard Electroweak Model*, edited by P. Langacker (World-Scientific, Singapore, 1994).
- [165] J.D. Jackson, S.B. Treiman and H.W. Wyld Jr., Phys. Rev. **106**, 517 (1957).
- [166] H. Behrens and W. Bühring, *Electron Radial Wave Functions and Nuclear Beta-decay* (Clarendon Press, Oxford, 1982).
- [167] S. Weinberg, Phys. Rev. **112**, 1375 (1958).

- [168] B.R. Holstein, Phys. Rev. C **29**, 623 (1984).
- [169] P. Herczeg, Phys. Rev. D **34**, 3449 (1986).
- [170] P. Herczeg, Prog. Part. Nucl. Phys., **46**, 413 (2001).
- [171] M.A.B. Bég, R.V. Budny, R. Mohapatra and A. Sirlin, Phys. Rev. Lett. **38**, 1252 (1977).
- [172] J. Ertler and M.J. Ramsey-Musolf, arXiv:hep-ph/0404291.
- [173] A. Sirlin, Rev. Mod. Phys. **50**, 573 (1978).
- [174] I.S. Towner, Nucl. Phys. **A540**, 478 (1992).
- [175] I.S. Towner, Phys. Lett. **B333**, 13 (1994).
- [176] S. Ando, H.W. Fearing, V. Gudkov, K. Kubodera, F. Myhrer, S. Nakamura and T. Sato, Phys. Lett. **B595**, 250 (2004).
- [177] H. Behrens and J. Jänecke, *Numerical Tables for Beta Decay and Electron Capture*, Landolt-Börnstein, New Series I/4 (Springer-Verlag, Berlin, 1969).
- [178] A.R. Edmonds, *Angular Momentum in Quantum Mechanics*, (Princeton University Press, 1964).
- [179] H. De Vries, C.W. De Jager and C. De Vries, Atomic Data and Nucl. Data Tables **36**, 495 (1987).
- [180] M.E. Rose, Phys. Rev. **49**, 727 (1936).
- [181] J.J. Matese and W.R. Johnson, Phys. Rev. **150**, 846 (1966).